FORMABILITY EVALUATION OF EN-10149-2STEEL SHEET METALUNDER IN-PLANE PLANE-STRETCHING CONDITION

A thesis submitted

By

Dereje H/Georgis

[GSR/0082/09]

For the Partial fulfilment of the Requirement for the award of degree of

Master of Science **in Manufacturing Engineering**

Under the Supervision & Guidance of

Dr. Perumalla Janaki Ramulu (PhD) and

Dr. Habtamu Beri (PhD)

Mechanical Design & Manufacturing Engineering Program

School of Mechanical, Chemical and Materials Engineering

Adama Science and Technology University

Adama, Ethiopia

September, 2018

ADAMA SCIENCE AND TECHNOLOGY UNIVERSITY

School of Mechanical Chemical and Material Engineering

Program of Mechanical Design and Manufacturing Engineering

Formability Evaluation of EN-10149-2 Steel Sheet Metal under In-Plane Plane-Stretching Condition

By

Dereje H/Georgis [GSR/0082/09]

Approved by Board of Examines

Approved by Board of Examiners

Chairman, Department Graduate Committee	Signature	Date
Major Advisor	Signature	Date
Co-Advisor	Signature	Date
Internal Examiner	Signature	Date
External Examiner	Signature	Date

Candidate Declarations

I hereby declare that the work which is being presented in this thesis entitled “Formability evaluation of High strength Steel material EN 10149-2 steel sheet metal under in-plane plane stretching Condition’’ in partial fulfillment of the requirements for the award of the degree of masters of science in Manufacturing Engineering is an authentic record of my own work carried out September 2016 to September 2018 under the supervision of Dr. Perumalla Janaki Ramulu, and Dr. Habtamu Beri, Program of Mechanical Design and Manufacturing Engineering, Adama science and Technology University, Ethiopia.

The matter embodied in this thesis has not been submitted by me for the award of any other degree or diploma. All relevant resources of information used in this thesis have been duly acknowledged.

Dereje H/Georgis Tefera	_______________	______________
Candidate	Signature	Date

This is to certify that the above declaration made by the candidate is correct to the best of myknowledge and belief. This thesis has been submitted for examination with our approval.

Dr. P. Janaki Ramulu	________________	________________
Advisor	Signature	Date
Dr. Habtamu Beri	________________	________________
Co-Advisor	Signature	Date

Acknowledgement

Thanks God, I barely finish my study without your help and your strength that comes from you. To be able to accomplish this study, I have been supported and supervised by many people that God sent to me. I thank my parents for the constant encouragement to pursue my dreams. Without the support of my wife, Miheret F., I would not have successfully reached this goal. I am very grateful for her enduring love throughout the whole process and for her patience and encouragement. To our new family addition, Bereket Dereje thanks for providing a big incentive to finish this study.

I believe that I would not be able to name everyone separately and to thank for everything that they did for me. However, I would like to express a few words of thanks from the bottom of my heart. I would like to express my deepest gratitude to:

DR. PERUMALLA JANAKI RAMULU, Advisor, I thank him for his great dedication and valuable suggestions which make me strong to step up beyond my deficiency. I would also like to thank him for his helpful guidance and continual sharing of knowledge, his intellectual support and advice makes me possible to accomplish this research works.

DR. HABTAMU BERI, Co-Advisor, for his valuable advising, inspiration, trust and vision to me to struggle the completeness of this work. I am thankful to him for his support.

My appreciation goes to Ayalew, Liyew and Daniel who are technicians at Ethiopian Conformity Assessment Enterprise for their unforgettable help during the samples testing.

I thank my classmates and colleagues of the ASTU, Manaye M., Kemal R, for their assistance and sharing information the way they perform before me. I also want to express great thanks to the MDME store keeper Yilikal Dinkayehu and Senior Academics and Research Assistants, Yared G.Michael at MDME, and Demeke Tesfaye at MSEfor their dedicative and useful support atthe workshop and experiment laboratory.

Specially, I would like to thank my wife's mother, Etagegn F.and my little sister Hirut A. for their endless encouragement and support.

I would like to thank all those too numerous to mention here, who have assisted and encouraged to complete my work.

Abstract

Metalworking processes are majorly grouped into two classes such as bulk-forming and sheet metal forming. In the sheet metal forming, blank is plastically deformed into the three-dimensional shape without critical changes in sheet thickness. In order to deform the sheet material to different formed object, the forming limit strains are mandatory for any metallic sheet. The present thesis work is aimed to evaluate the forming limit strains of the EN-10149-2 steel sheet metal of 2.42mm thickness under In-Plane Plane-Stretching condition at ambient conditions. EN-10149-2 Steel has good mechanical properties and light weight that increase the application in automotive, aerospace, and Industrial structural design compared to other metals. For which, the tensile and plain stretching test samples were prepared in three rolling direction 0°, 45° and 90°. The mechanical properties of EN-10149-2 steel are evaluated from the tensile testing such as the yield strength, tensile strength, uniform elongation, total elongation, hardening exponent (n-value), material strength coefficient (K) and plastic strain ratio (R-value).The microstructure and hardness of the material were also evaluated. In-plane plane-stretching evaluation test has been carried out by stamping circular grids at middle of the specimen by which measured the minor and major strain using thickness gradient necking criterion (TGNC). For validation of the results, simulations were performed using PAM STAMP 2G a finite element code. The obtained results from experiments and simulations found that the maximum limit strain is appeared for the rolling direction of 45° and followed by the 90° and 0°. This indicates that the maximum formability is in 45° rolling direction during in-plane plane-stretching test. Both experimental and Simulation results in-terms of limit strains from in-plane plane-stretching test on EN - 10492-2 steel sheet metal are in an acceptable error percentage of 5 to 8 %.

Keywords: forming limits strain; IPPS; TGNC; Mechanical Properties Circular Grid; Major and Minor Strain.

Tables of Content

Page No.

List of Tables

List of Figures

List of Abbreviation

AHSS	*Advanced High Strength Steel*
HSLA	*High Strength Low Alloy*
ASTU	*Adama Science and Technology University*
MTEC	*Metal Engineering Corporation*
HMMB	*Hibret Manufacturing and Machine Building Industry*
RD	*Rolling Direction*
DD	*Diagonal Direction*
TD	*Transverse Direction*
FLD	*Form Limit Diagram*
FLC	*Forming Limit Curve*
ULC	*Upper Limit Curve*
LLC	*Lower Limit Curve*
AISI	*American Iron and Steel Institute*
ASTM	*American Standard Testing Method*
FFL	*Fracture Form Limit*
FE	*Finite Element*
LDH	*Limit Dome Height*
UTS	*Ultimate tensile strength*
UE	*Uniform elongations*
YS	*Yield strength*
HV	*Vickers Hardness Number*
IPPS	*In-plane Plane Strain*
TGNC	*Thickness Gradient-based Necking Criteria*

List of Acronyms

ε_1	*Major strain*
ε_2	*Minor strain*
β	*strain ratio*
e	*Engineering strain*
s	*Engineering stress*
ε	*True strain*
F	*maximum load*
n	*Work hardening exponent*
r	*Anisotropy factor*
k	*Materials strength coefficient*
ΔL	*Change in length*
l_0	*Original gauge length*
σ	*True stress*
m	*Strain rate sensitivity*
τ	*Shear stress*
$\bar{\sigma}$	*Equivalent stress*
ε_w	*True width strain*
ε_t	*True thickness strain*
w_f	*Final width*
w_o	*Original width*
t_f	*Final thickness*
t_o	*Original thickness*

CHAPTER ONE

1. INTRODUCTION

1.1. Sheet metal forming

Generally, Metalworking is defined as the process of deforming a metal billet or blank into required shape and size using tools or dies. The characteristics of the work piece material, mechanics of plastic deformation (metal flow), the conditions at the work piece - tool interface, and the equipment used and finished product requirements are the main influence on design and control of metalworking [1]. It is one of the real advancements to manufacture metal parts and the most seasoned and most develop metal segments' creation technique. There were parcel of advancement of new kinds of metal working equipment and new materials with exceptional properties and applications in the past 100 years. In metalworking, at first a basic part like billet or a blanked sheet is plastically deformed between tools to obtain the desired final configuration [2].

Basically, metalworking processes are grouped into two classes namely bulk-forming and sheet metal forming. The sheet metal blank is plastically deformed into a three-dimensional shape, regularly without critical changes in sheet thickness. More often than not, the shape of the work piece is subjected to change however the cross-sectional area isn't changed much. In some cases, elastic recapturing or spring back may be significant because the magnitudes of plastic and elastic deformations are comparable. Some of the important sheet metals forming processes are deep drawing, stretching, bending and rubber pad forming [2].

The automotive industry of the 21st century demands the use of cutting edge materials and manufacturing technology. The need for lightweight high strength materials increases as automotive manufacturers are driven to continually produce superior automobiles that have improved performance, higher fuel economy, and improved safety. This need continues to drive the vehicles' material selection process. Improvements in the design of a vehicle's chassis in particular are now being realized through the use of new materials and manufacturing processes. There is one drawback, however; high strength steels have lower formability. It is well known that as materials increase in strength their formability typically decreases. Figure 1.1 illustrates the elongation versus strength for various automotive grade steels. The graph shows a decrease in material elongation with increased strength. Though elongation is not a complete measure of formability, the graph in Figure 1.1 demonstrates the formability trend for each of the materials shown [3].

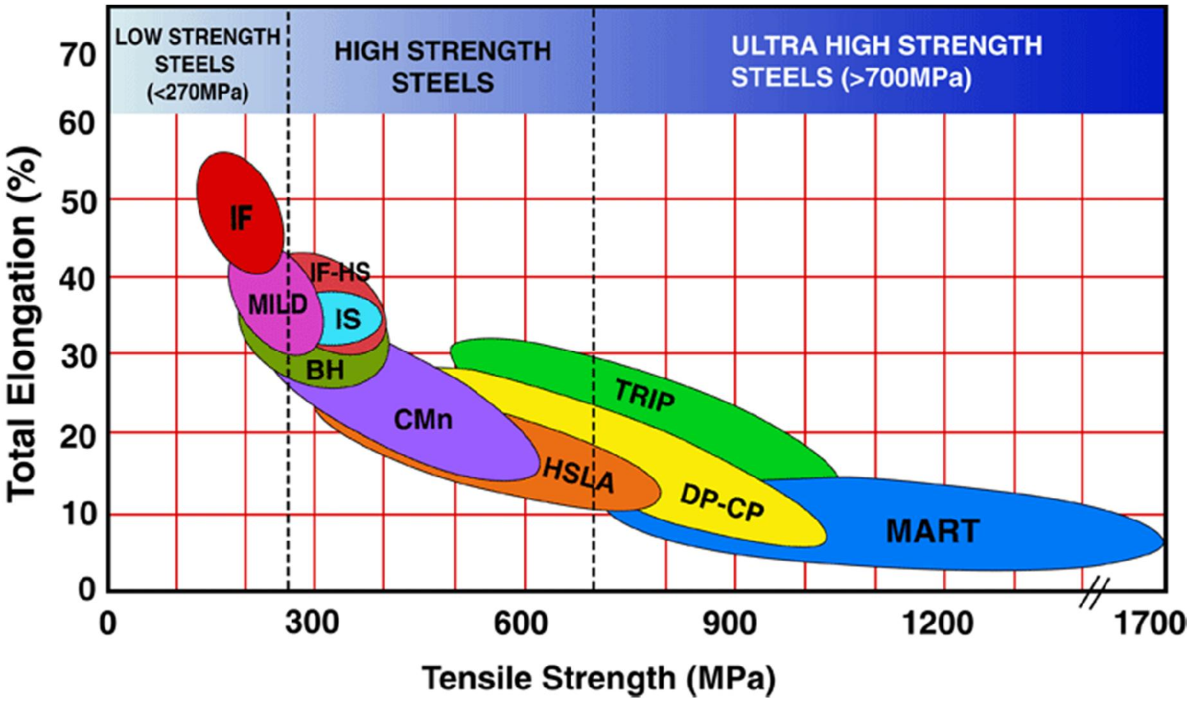

Figure 1. 1 Comparison of steels [3]

Moreover, numerous car businesses vehicles composed under thought of light weight, crash execution, vitality sparing, and ecological perspective are of unique intrigue. Using steel sheets with reduced thicknesses is desired as they lead to lower fuel consumption. However, at the same time, passenger safety must be achieved by applying steels with an increased ability of energy absorption. This need continues to drive the vehicles' material selection process. Improvements in the design of a vehicle's chassis, in particular, are now being realized through the use of new materials and manufacturing processes. Steel industries are also developing new grades of Advanced High Strength Steels (AHSS) with high strength to weight ratio as lightweight structures [3].

In 1958, the primary business arrangement of high strength low alloy (HSLA)(High quality low combination) steels called GLX-W with Niobium (Nb) was delivered by the National

Steel Corporation of the United States [4]. These illustrations speak to, maybe, the disclosure arranges and the business presentation of a group of steels that has in this manner come to be known as HSLA steels. The composite plan logic and thermo-mechanical handling important to improve the microstructure property connection of HSLA steels can be viewed as a standout amongst the most problematic innovations in the steel business. The enthusiasm of utilizing HSLA steels in the car business turned into a need because of the oil emergency in 1973. The business was looked with the test of diminishing the heaviness of vehicles to diminish fuel utilization [5].

In Ethiopia, other than advanced high strength steel (AHSS), EN - 10492-2 steel sheet metalsheet metal applied in different steel manufacturing industries. Some of these are Metal Engineering Corporations [METEC] and HibretManufacturing and Machine Building Industry [HMMBF], they have been manufactured different machinery component and structures. So that, the researcher believed that it is useful to study formability limits based on in-Planestretching tensile test of the selected HSLA steel sheet metal.

1.2. Statement of the problem

Although many studies have been investigated the formability of High strength Steel both experimentally and numerically but the formability of EN - 10492-2 steel sheet metal under in-plane stretching condition has been studied rarely. Studiespublished so far described the formability prediction based on the strain path diagrams, yield criteria but a detailed description of the formability of EN - 10492-2 steel sheet metalwith 2.42 mm thickness under In-Plane Plane-Stretching (IPPS) condition has not discussed much.Based on the applications of the EN - 10492-2 steel sheet metal at different level industries, the present thesis work will generate the data for forming characteristics of this particular material

1.3. Objectives of the Study

1.3.1. General Objective

The general objective of this work is to evaluate the formability of EN 10492-2 steel sheet metal under In-Plane Plane stretching condition using experiments and numerical simulations.

1.3.2. Specific Objectives

The specific objectives are as follows:

- Evaluate the mechanical properties of the material through tensile testing.
- Determine the strains occurred in EN - 10492-2 steel sheet metal during in-plane plane-stretching testing
- Evaluate the formability of EN-10149-2 sheet metal in-plane stretching after testing.
- For Validation, Simulate the process for formability of EN-10149-2steel sheet metals using Finite element software.
- Comparing Experimental and Numerical results for validation.

1.4. Scope of the Study

The scope of this thesis work is to focus only the experimental and numerical formability prediction of EN-10492-2 steel sheet metal under in-plane Stretching conditions. The forming conditions are regarding at room temperature. The numerical simulation will do by using a Finite element of PAM-STAMP-2G software. Also, the mechanical property such as tensile test and plane strain tension test at 0^0, $45^0$and 90^0 with rolling direction of EN-10492-2 steel sheet metals will be evaluated under in-plane Stretching condition..

1.5. Significance of the study

The significance of proposed project is as follows:

- It contributes for the global automotive industries as an alternative method.
- This research output can be used as initial input for automaker and manufacturing industries in Ethiopia.
- To enrich and practice for the researchers their theoretical and practical knowledge.
- After the completion of this work the data can be used directly without any formability tests.
- It will be a very good reference for further study on formability prediction method of steel metals and for any interested individuals.

1.6. Thesis Organization

The body of the thesis is presented in the following five chapters:

- **Chapter 1** Introduce the general background bout sheet metal forming and the history of HSLA steel,
- **Chapter 2** provides a review of relevant literature, including: sheet metal formability, experimental and numerical method of sheet formability evaluation in plane stretching test and the parameters affecting strain path effects.
- **Chapter 3** summarizes the materials employed in this study along with their mechanical properties and microstructures. And also discusses the experimental procedure used for this research, detailing the test apparatus and sample geometries employed.
- **Chapter 4** presents the results and discussion of the results as well as a comparison that has been obtained through the experimental testing with numerical analysis completed in this study.
- **Chapter 5** summarizes the conclusions drawn from this research and offers some recommendations for improvements in the methodology.

CHAPTER TWO

2. LITERATURE REVIEW

2.1. Introduction

A fundamental problem in sheet metal forming is fracturing. Especially as the strength of the steel sheet metals increase its formability becomes decreased or limited small scale. It is therefore essential to be able to predict the risk of fracture and forming limit with high accuracy[6]. This chapter provides a literature review concerning previous research on determining a given sheet material formability to be a guideline to run this study. It describes the different testing carried out and measurement methods that have been being used to evaluate the formability of the material. It will also discuss how multiple or varying strain paths affects sheet material formability. It also gives a contextual understanding of the in-Plane stretching test method which was simulated for sheet metal sample testing in this entire study. Finite element technique has been performed on sheet metal forming analysis to obtain accurate results. It had also discussed the concept of sheet formability, types of sheet metal formability test, factor influencing forming limit strain and FE method.

2.2. Sheet Metal Formability

The formability of sheet metal can be defined as the capability of sheet metal to undergo plastic deformation to a given shape without defects or fractures. And it is characterized by the principal strains that are produced in the sheet as a result of various forming operations. The major and minor principal strains often correspond with the rolling and transverse sheet directions (RD and TD).Each type of sheet metal can be deformed only to a certain limit that is usually imposed by the onset of localized necking, which eventually leads to the ductile fracture. The standard and well-known approach for quantifying limit is the forming limit diagram (FLD),which is a graph of the major strain (ε_1) at the onset of localized necking for all values of the minor strain (ε_2)obtained in the plane of the sheet material in2D strain space[7].

The diagram split into two sides; “left side” and “right side”. The first diagram, right side, was presented by Keeler and Backofen that was just positive major and minor strains are plotted as appeared in Fig. 2.1.Keeler recommended that amid forming the initial circles of the grid become ellipses. It plotted the major strains against the minor strains got from such ellipses at fracture of parts after biaxial stretching ($\varepsilon_1 > 0$; $\varepsilon_2 > 0$)[8].

Later, Goodwin GM, completed the FLD by adding the left side, with positive Major and negative Minor Strains plotted the curve for the tension/compression domain ($\varepsilon_1 > 0$; $\varepsilon_2 < 0$) by using different mechanical tests as show in Fig. 2.2. Various strain paths can be generated in order to create different combinations of limiting Major and Minor Strains. The "left side" represents strain paths with strain[9].

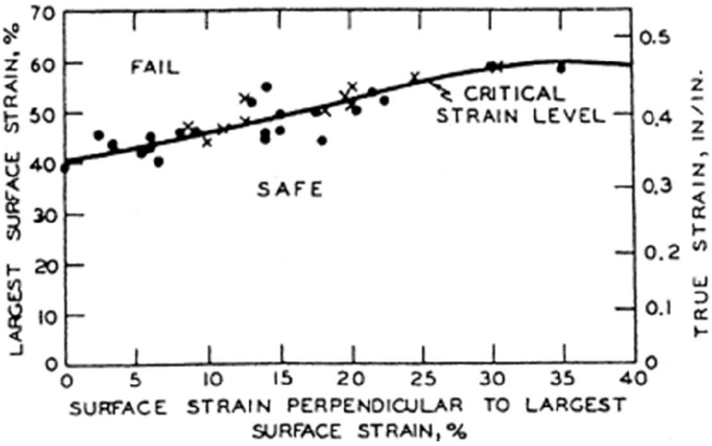

Figure 2.1 Forming Limit Diagram defined by Keeler[8]

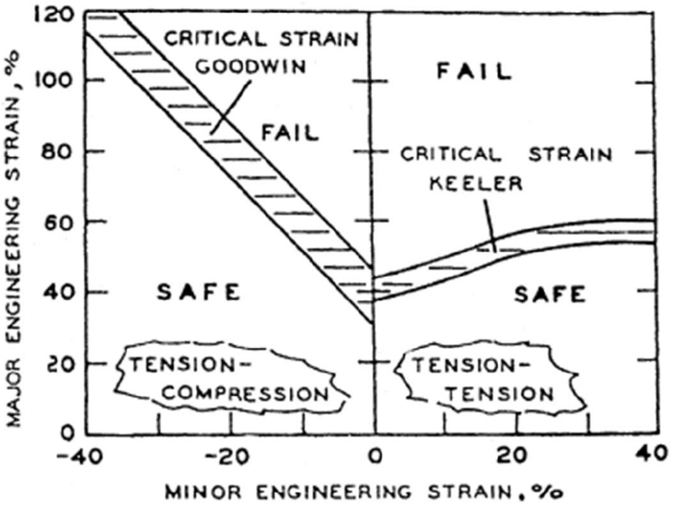

Figure 2.2 Forming Limit Diagram defined by Keeler and Goodwin[9]

These strains can be represented as either engineering or true strains. The limiting strains on an FLD form a threshold which is known as the forming limit curve (FLC). A schematic of forming Limit diagram with various strain paths is given in Fig.2.3.Asshownin Fig.2.3, thFLD is constructed based on the strain paths obtained from biaxial stretching experiments on different sample geometries. The region under the curve is considered to be safe for any particular deformation mode, while everything above the FLD curve is considered to be potential for fracture. Sometimes, another curve, which is called a safe FLD curve, is plotted 10% below the FLD. A higher FLD curve indicates that the material has greater formability. The FLC represents a boundary between the safe and failed forming regions on an FLD. The safe region is represented by the area below the curve where the material does not exhibit visible necking. The failed region refers to the area above the curve where the material has begun to form a visible (local) neck; hence, the material begins to lose its strength[1].

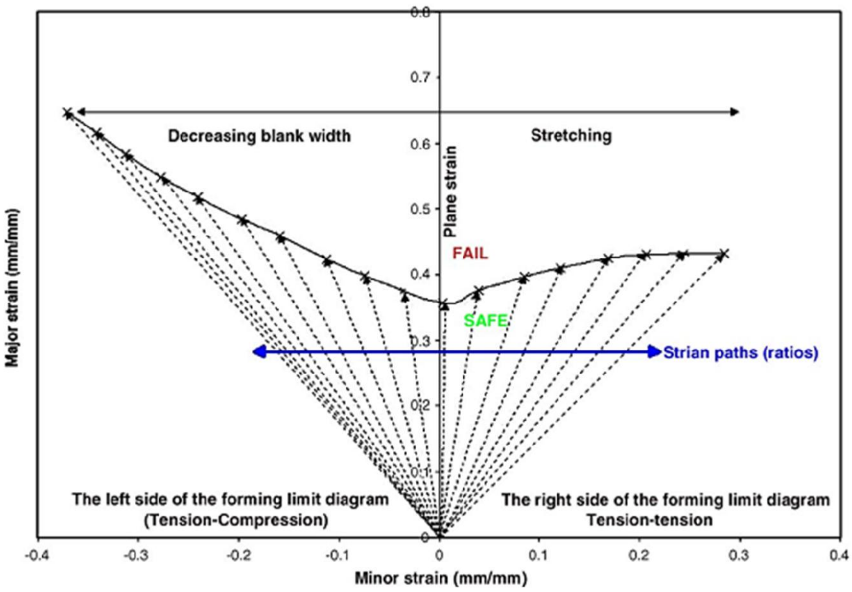

Figure 2.3 A schematic of forming limit diagram [10]

The FLC on an FLD represents a wide range of forming limit strains that are predicted when sheet material is deformed along linear strain paths. These strain paths range from uniaxial tension to plane strain to equi-biaxial tension, as illustrated in Figure 2.4, which shows an example of a theoretical FLD plotted in terms of true strains, rather than engineering strains [11]. These linear strain paths can be described by the ratio of minor true strain (ε_2) to major true strain (ε_1) where:

$$\beta = \frac{\varepsilon_2}{\varepsilon_1} ------------------ 2.1$$

Where; β is the strain path ratio, and ε_1, $\varepsilon_2$are minor and major true strain respectively.

So that, the strain path where -0.5 <β< 0 results in drawing of the sheet material. When β ≈ 0, acondition of plane strain is achieved and when 0 <β< 1, the material is stretched inbiaxial tension.

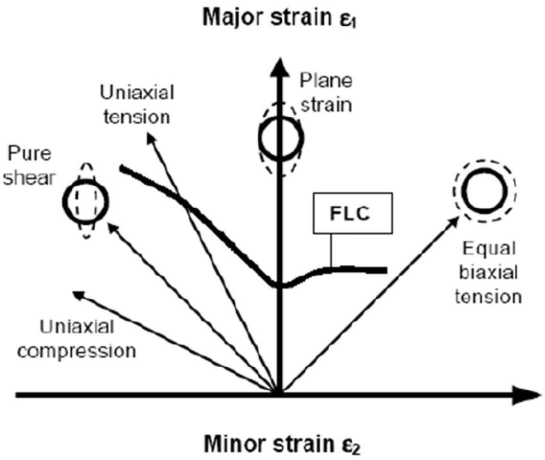

Figure 2.4 A typical FLD showing various linear strain paths [11].

2.3. Experimental Determination of the Forming limits strains

The FLD diagrams are established by experiments that provide pairs of values of the limit strains ε1 and ε2 obtained for various loading patterns (equi-biaxial, biaxial, uniaxial etc.).The limiting strains on an FLD can be either determined experimentally or predicted analytically. Experimentally, an FLD is determined from a grid of circles, lines or dots that has been applied to the surface of the sheet sample before the forming operation. These grids provide a basis for the measurement of local strains. The deformed grids are measured and then compared to the original grid size to determine the principal strain levels. The grids can be applied using different techniques, typically electrochemical etching, silk screen printing, and rubber stamp [12-15].

Normally, forming limit strains are determined experimentally by performing either out-of-plane or in-plane forming tests on flat sheet samples. For clarity, the plane being referred to is the plane made by the Rolling Direction (RD) and Transverse Direction (TD) of the material. The more conventional out-of plane forming test typically uses a 4-inch diameter hemispherical punch to form a dome in sheet metal samples that are clamped around their circumference as shown in Figure 2.5. The hemispherical punch deforms the material out-of-plane creating a curved surface on the sheet specimens, which makes the measuring of deformed grids more difficult. Thus, the concept of performing in-plane formability tests was first adopted by Marciniak and Kuczynski to allow deformed grids to be measured all on one flat surface [17].

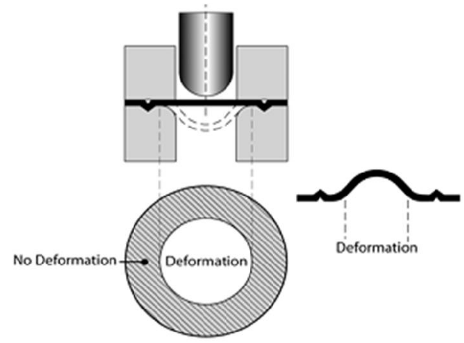

Figure 2.5Hemispherical dome punch test setup consisting of a circular specimen that is clamped between two dies resulting in out-of-plane deformation [16].

Their in-plane forming test employed a flat punch that deformed the sample indirectly by applying pressure through a circular washer to reduce friction from the punch, allowing the material at the center of the sample to deform freely. Figure 2.6 illustrates the in-plane test setup used by Marciniak and Kuczynski.

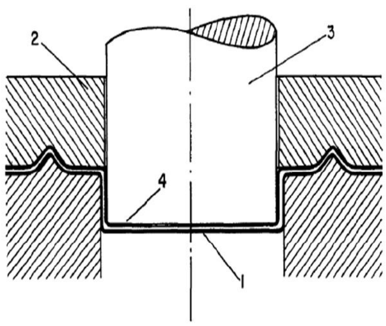

Figure 2.6. Flat bottom punch 3, used to indirectly apply pressure to a specimen 1, through a circular washer 4, deforming the material in-plane. The sample and washer are clamped rigidly in a die, 2 [17].

The sample geometry required to produce a given strain path on an FLD varies according to the strain path. Figure 2.7 shows examples of the sample geometries and dimension to produce strain paths ranging for uniaxial tension forming tests. The thinnest samples, shaped like an hour glass, are used to generate uniaxial strain paths, for obtaining different strain paths, specimens with different shapes and sizes with and without notches are used. This test allows determining a section of the FLD in the range $\varepsilon_2 < 0$.

The advantages of the tensile test for determining FLDs are that the specimens are easy to manufacture and a general purpose testing machine can be used; furthermore the specimens remain plane during the test which facilitates measurement. However, only the negative section of the forming limit diagram ($\varepsilon_2 < 0$) can be determined [18].While the widest square samples are used to generate equi-biaxial tension. The rest of the samples are needed to generate the various strain paths in between these two extremes. Several researchers [19-23], have shown that by varying the sample geometry, forming limit strains can be obtained for all linear strain paths on an FLD from uniaxial tension to equi-biaxial tension.

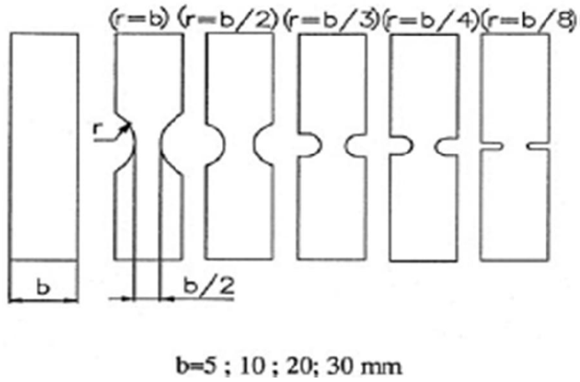

Figure 2.7 Rectangular specimens with and without notches [18]

2.3.1. Out-of-plane vs. In-plane

Even though in-plane forming tests show a significant advantage in allowing strains to be measured on a flat surface, out-of plane forming tests are still used as the industry standard method for evaluating sheet material forming limits. However, limit strains produced from out-of-plane forming tests have been shown to depend on the tooling geometry and friction [22, 28]. Variables such as punch radius and lubrication types' have a significant effect on out-of-plane forming test results. Lewison and Lee and Raghavan, have developed modified Marciniak and Kuczynski (MK) tests that allow the sample material to deform freely "in plane" with less effect of tool geometry and friction[19, 22].

Lewison and Lee and Raghavan have continued research using similar in-plane forming tests. These in-plane forming limit tests showed that the material forming limits were more sensitive to the defects within the material [19 - 22] than with tool geometry and friction. Lewison and Lee performed a comparison study of out-of-plane vs. in-plane forming tests and found that the out-of-plane tests produced forming limit strains that were 4-8% higher than in-plane tests on the same sheet material.

This effect was also reported by Raghavan along with Ghosh andHecker who all agreed that geometric constraints imposed by the tooling used in out-of-plane tests delays the localization of limit strains, thereby resulting in higher forming limits compared to in-plane tests[19, 22, and 23].

To eliminate all effects of tooling geometry and friction, a few researchers [9, 23-26], have suggested methods for performing in-plane forming limit tests using purely tensile forces. The benefit is that these tests can be carried out using standard tensile testing machines, which eliminates the need for specialized press forming equipment. However, these tensile deformation methods are capable of producing strain paths only on the left hand side of the FLD, ranging from uniaxial tension to plane strain.

2.3.2. Strain Measurement

The strains that develop during a sheet material forming limit test can be collected either by manually measuring the deformed grids by hand or using computer driven image processing software to calculate the resultant strain from still pictures. In both cases, in-plane forming tests allow the deformed grids to be readily measured. The measurement of localized strains produced from an out-of-plane hemispherical dome test is considered to be the most popular way in determining sheet metal FLDs. However, these measurements are typically obtained through hand inspection using transparent tape and a magnifier or another optical device such as a microscope [27]. This method is very subjective especially when the measurements are conducted by different individuals.

Lewison and Lee carried out in-plane forming limit tests to compare the strain levels from aluminum killed drawing quality (DQ) steel specimens that were calculated from visually inspected still images versus those obtained through digital imaging analysis software. They concluded that local necking can be detected by digital image analysis before it can be visually seen or identified by touch. Thus, the use of digital image analysis can be a more reliable and accurate method for capturing sheet material forming limits [19].

When using digital image analysis to capture the forming limit strains, the resolution of the recording device is paramount. A camera with insufficient resolution will produce large statistical errors in the measured strain results, while a camera with too high resolution will cost more and require more processing power. It discovered that when he performed in-plane forming limit tests using a digital video camera with a resolution of 640x480 pixels that the experimental error in his strain measurements was ± 2% engineering strain for a 95% confidence interval.

2.3.3. Thickness gradient-based necking criterion (TGNC)

A novel thickness gradient-based necking criterion is used to obtain FLC in the present work 29[53]. In general, necking can be understood as a thinning phenomenon. Nandedkar 29[53] developed this novel criterion and it basically perceives necking as a localized thinning phenomenon i.e., a localized region within the deforming sheet where a steep gradient in thickness develops. A local critical thickness gradient (Rc) must exist at the onset of a local visible neck. In the simulations, the thickness gradient developing in the adjoining elements (of size about 1–5 mm) is monitored, and, when this gradient (Ractual) drops below a critical value, it is concluded that the local neck has initiated in the element where thickness is lower.

The maximum major and minor strain in the thinner element is then reported as the forming limit strain of that particular deformation condition. It is found from the earlier experiments that necking occurs in the sheet metal when the thickness gradient (ratio of thickness of neighboring elements or circles) falls below 0.92 29[53].. The schematic of applicability of this criterion is shown in Fig. 4.13. This limit strain theory is sensitive to 'mesh size'. From the previous study, it was found that the mesh size should be 2–5 mm to follow this criterion, which is equivalent of what is followed in experimental determination, wherein 3 mm circle grids are etched on sheet surface. In the present work, a uniform mesh size of 2 mm is used in simulation.

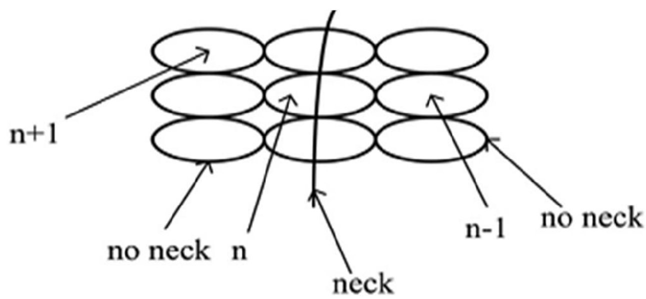

$$R_{\text{thickness gradient}} = \frac{\text{thickness}_{\text{Necking element}}}{\text{thickness}_{\text{Neighboring element}}} = \frac{t_n}{t_{n-1}} \, or \, \frac{t_n}{t_{n+1}} \leq R_{\text{Cri}} \Rightarrow \text{material failure or necking}$$

$$\text{R}_{\text{Critical}} = 0.92$$

Figure 4. 1Schematic representations of deformed grids and applicability of thickness gradient-based necking criterion

2.4. Theoretical Forming Limit Criteria

Critical levels of deformation, so-called sheet forming limits, can be characterized by both the diffuse necking and the local necking states. Diffuse necking occurs when uniform deformation stops, as the material reaches its maximum strength. The local necking condition is reached when the strain rate in any one sheet direction reduces to zero [30].

Following Hill, it can be shown that in a uniaxial tension test, diffuse necking corresponds to deformation at the point of maximum loading (dF = 0), otherwise known as the *A. Considère condition* ,and it is given by:- [31].

$$\sigma_1 = \frac{d\sigma_1}{d\varepsilon_1} ---------------------- 2.2$$

Assuming that the material is plastically isotropic and can be represented by a Hollomon power-law hardening model which is given by:[37]

$$\sigma_1 = K{\varepsilon_1}^n ---------------------- 2.3$$

Where K is a constant and n is the strain hardening exponent, Equation 2.3 can be substituted into Equation 2.3 to produce:

$$\varepsilon_1 = n ----------------------- 2.4$$

Equation 2.3 predicts the diffuse necking criterion in terms of true strain. This equation demonstrates the effect that the strain hardening exponent, n, has on delaying the onset of diffuse necking. In fact, it can be shown that regardless of strain path (i.e. from uniaxial tension to equi-biaxial tension), the onset of diffuse necking occurs when Equation 2.3 is satisfied.

For local necking, Hill suggested that this condition occurs in sheet material when the true strain rate in some characteristic direction in the plane of the sheet reduces to zero, $d\varepsilon_2 = 0$.

Thus, the magnitude of the through-thickness strain is equal (but opposite in sign) to the major principal strain in the plane of the sheet [32]. For an isotropic material under uniaxial tension the through-thickness strain increment is represented as:

$$d\varepsilon_3 = \frac{d\varepsilon_1}{2} ---------------------- 2.5$$

The Considère condition must also be satisfied for local necking to occur. Thus the local necking criterion is satisfied in a uniaxial tensile test when:

$$\frac{d\sigma_1}{\varepsilon_1} = \frac{\sigma_1}{2} ---------------------- 2.6$$

By substituting Equation 2.5 into Equation 2.3 Hill demonstrated that the local necking criterion for a power-law hardening material tested under uniaxial tension is given by:[37].

$$\varepsilon_1 = 2n ---------------------- 2.7$$

Hill's [33] local necking theory can only be applied to the range of strain paths on the left hand side of an FLD from uniaxial tension to plane strain. This local necking condition can be found by evaluating:

$$\varepsilon_1 = \frac{n}{(1+\beta)} ---------------------- 2.8$$

Where; - $\beta \leq 0$ (left-hand side of FLD). Figure 2.3 shows the diffuse and local necking theories predicted by Hill compared to an experimental FLC [30, 32]. It is evident that the local necking curve predicted by Equation 2.8 shows the same trend as a typical experimental FLC.

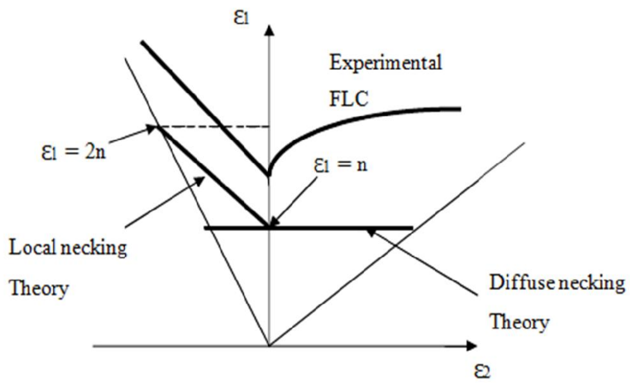

Figure 2.8 A FLD showing the predicted limits given from both the diffuse and local necking theories proposed by Hill compared to an experimental FLC. [30, 32]

2.4.1. Plastic Anisotropy

Plastic anisotropy is related to the crystallographic texture of a material's microstructure after it has under gone processing (e.g., rolling or annealing). It is a measure of the preferred grain orientations in the material and how they react under deformation. It can be represented as either normal or planar anisotropy. Normal anisotropy measures a material's ability to resist thinning during a uniaxial tension test using the Lankford parameter:

$$r = \frac{\varepsilon_w}{\varepsilon_t} -------------------- 2.9\ [30]$$

Where; - ε_w, ε_t, are the strains in the width and thickness directions, respectively. The r-value is typically measured in the 0º, 45º and 90º sheet directions. Planar anisotropy is a measure of how the r-value varies with respect to the different sheet directions.

Up to this point, necking has been described based on assuming isotropic material properties. In many sheet materials this is not the case, and an anisotropic material model is required. If anisotropic material properties are considered it can be shown that Hill's local necking theory given in Equation 2.7 can be rearranged to give:

$$\varepsilon_1 = (1 + r)n -------------------- 2.10$$

2.5. Analytical Sheet Forming Limit Prediction

Forming limits can be predicted analytically using an approximation first described by Keeler and Brazier. They suggested that the forming limits in sheet steels can be predicted by a characteristically shaped curve plotted on a standard FLD. Figure 2.9shows a standard FLD with the calculated Keeler-Brazier FLC plotted using true strains [34].

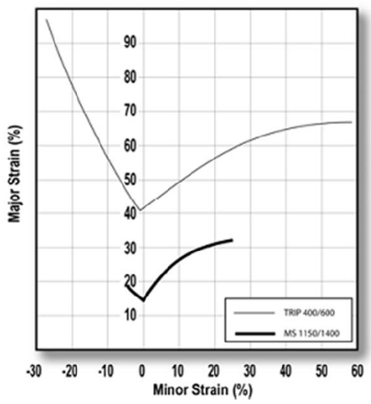

Figure 2.9 Preliminary experimental FLCs for t=1.2 mm TRIP steel and t =1.5 mm MS steel [16].

The reference point for a predicted FLC is the value of the true plane strain forming limit, FLC0, which can be estimated based on sheet thickness, t (mm), and the strain hardening coefficient, n, using the following equation:

$$FLC_0^{True\ Strain} = \ln\left\{1 + [23.3 + 14.2t] * \frac{n}{0.21}\right\} - - - - - - - - - - - - - - 2.11$$

The strain hardening coefficient, n, is determined at high strain levels, typically 15-20% (terminal n-value). The left hand side of the FLC is simply a straight line with slope equal to negative one that intersects the true plane strain forming limit, FLC0. The right hand side of the FLC is a specific curve generated by Keeler using stretch forming tests on low-carbon steel. Figure 2.10 shows an example of the FLC0 Engineering Strain predicted using the Keeler-Brazier approximation for a HSLA sheet steel. The Keeler-Brazier approximation is based on forming limit results that were obtained using out-of-plane hemispherical dome punch tests on various sheet steels.

Keeler had previously suggested that the formability of sheet metal was directly related to its thickness. Raghavan, reinforced this suggestion when he performed in-plane forming tests on different steel sheet thicknesses and found an increase in formability with increased thickness [35].Figure 2.10 shows the agreement of the predicted FLC_0 Engineering Strain with experimental forming limits plotted as major and minor engineering strains. The plane strain forming limit is useful to know for a given material because it is typically the path that would produce the least amount of strain, prior to failure.

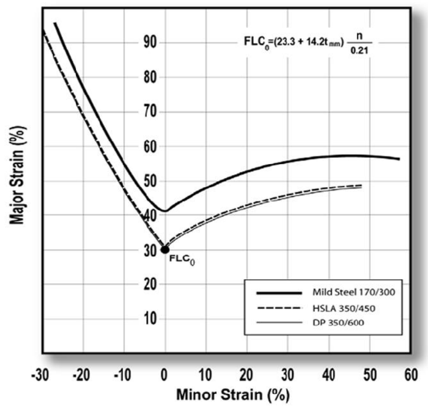

Figure 2.10 Experimental FLCs for one sample each of Mild, HSLA, and DP steels with thicknesses equal to 1.2 mm. [16]

2.6. In-Plane Tensile Testing

Wagoner and Wang were among the first researchers to develop in-plane tensile forming limit tests, which allowed them to produce strain paths between uniaxial tension and plane strain. Their experimental setup included a 254 mm wide grip assembly that relied on a bolted wedge to clamp the specimens. They began with a254 mm wide sheet sample of 2036-T4 aluminum, as shown in Figure 2.11, and varied the geometry of its gauge region in an effort to maximize plane strain throughout the sample. Their testing showed that plane strain deformation could be achieved across approximately 80% of the gauge region [36]. This testing procedure became known as an in-plane plane strain (IPPS) test.

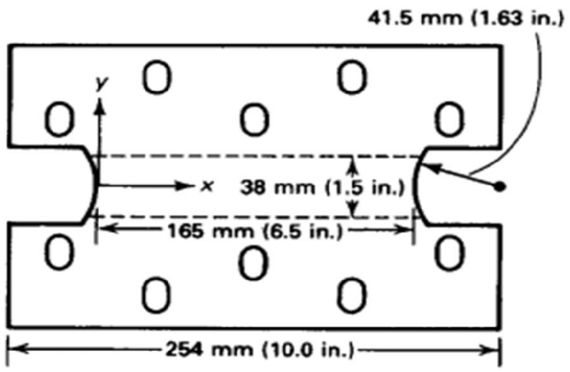

Figure 2.11 Wide sheet sample used for in-plane tensile deformation testing used by Wagoner and Wang [36]

Holmberg et al. developed in-plane tensile tests to produce strain paths from uniaxial tension to plane strain in mild steel and high strength steel. Their intent was to create an in-plane forming limit test that was independent of tooling geometry and friction. A sample of the geometry they employed is shown in Figure 2.13. They found that a wide sample with a wide but short gauge section is needed to produce forming limit strains close to plane strain. They also suggested that the sample have sufficient area for clamping to avoid fracture outside the plane strain region in the center of the sample [11].

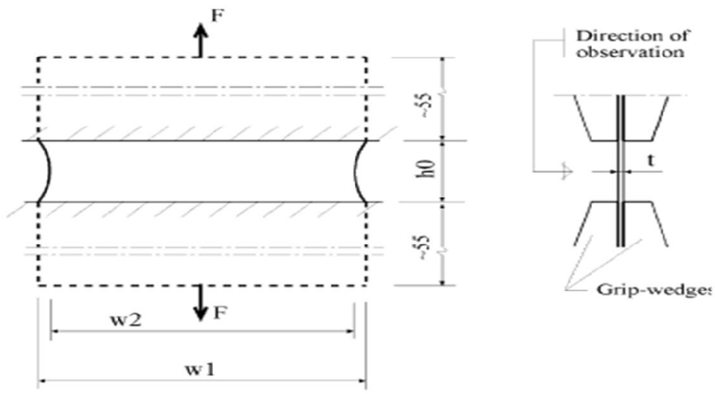

Figure 2.12 In-plane tensile test sample used by Holmberg et al. dimensions are in mm, h0 ranged from 6 to 12 mm, w1 and w2 ranged from 16 to 76 mm. [11]

Valletta et al. performed an IPPS tensile testing study by using LS-DYNA finite element method (FEM) software to predict the deformation behavior of DQ and DP600sheet steel for varying sample geometries under tensile loading conditions. Valletta's simulations showed that wide samples with an appropriate notch profile could be used to apply strain paths between uniaxial tension and plane strain to the DQ and DP steels. Valletta concluded that a wide sample with short gauge length is needed to produce strains close to plane strain at the center of the sample. Valletta's experimental IPPS tests used custom 104 mm wide grips on a standard Introns tensile testing machine to apply the tensile loads to sheet samples [37].

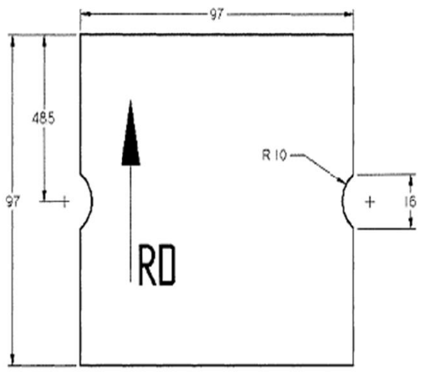

Figure 2. 13 The pre-strain test sample used by for pre-straining the DQ sheet steel

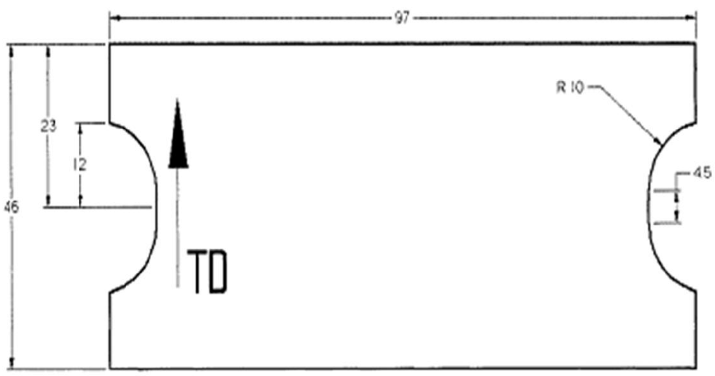

Figure 2. 14 The in-plane plane strain (IPPS) test sample for determining pre-strain effects on plane strain forming limits,

Concerning applications, the whole scope of high strength low alloy steels are reasonable for basic segments of autos, trucks and trailers, for example, suspension frameworks, skeleton, and support parts. High strength low alloy steels offer great exhaustion, torsion unbending nature, and effect qualities. Given these attributes, this class of steels offers weight decrease for support and auxiliary parts [38].

Likewise, EN - 10492-2 steel sheet metal sheet has many application areas in modern manufacturing industries. It has also good mechanical properties and light weight that increase the application in automotive, aerospace, and Industrial structural design compared to other metals. Main applications of EN - 10492-2 steel sheet metal are;-[39]

- Body and chassis components for the automotive and truck industry, bumper brackets, engine mounting brackets, passenger car components and wheel centers.
- Crane jibs and booms heavy-duty highway and off-road vehicles,
- A wide variety of uses for rolling stock, cold formed sections.
- Oil and gas pipelines,
- construction and farm machinery, industrial equipment, storage tanks, mine and rail-road cars, barges and dredges,
- Snow mobiles, lawn mowers, Bridges, off-shore structures
- Power transmission towers, Light poles, and building beams and panels are additional uses of these steels.

To sum up, any influence studied on formability of sheets material should be validated for a critical condition like plane strain deformation. Any further design issues on forming of steel sheets could be based on the effect studied and data evaluated through in-plane plane strain (IPPS) formability tests and not tensile tests. Another significant factor to be noted is that the IPPS sample design is simple and tests can be conducted in a universal testing machine, as the deformation is restricted to a single plane (called as 'in-plane'). The data obtained from the IPPS formability test is independent of friction and bending, unlike in out-of-plane tests such as limiting dome height tests and deep drawing, though plane strain deformation can be obtained in out-of-plane formability tests too. Moreover, out-of-plane formability tests require special purpose hydraulic machines; experimental setup (including punch, die and blank holder) and a complex sample design to perform experiments and evaluate formability.

CHAPTER THREE

3. MATERIALS AND METHODOLOGIES

3.1. Introduction

This study was performed to evaluate the formability of sheet metal and the parameters affecting this phenomenon, by using of experimental and simulation analysis. The aim of this section is to present the details of the experimental and FE simulation procedures that used in this study. A simple 2D plain stretching test process was investigated through FE simulations for EN-10149-2 steel sheet material. The effects of factors investigated in this study include; rolling directions and plastic anisotropy. For the FEM evaluation PAM-STAMP-2G software was used for all simulations. The detailed methodology was mentioned in the Fig. 3.1 in the form of flow chart.

3.2. Project flow chart

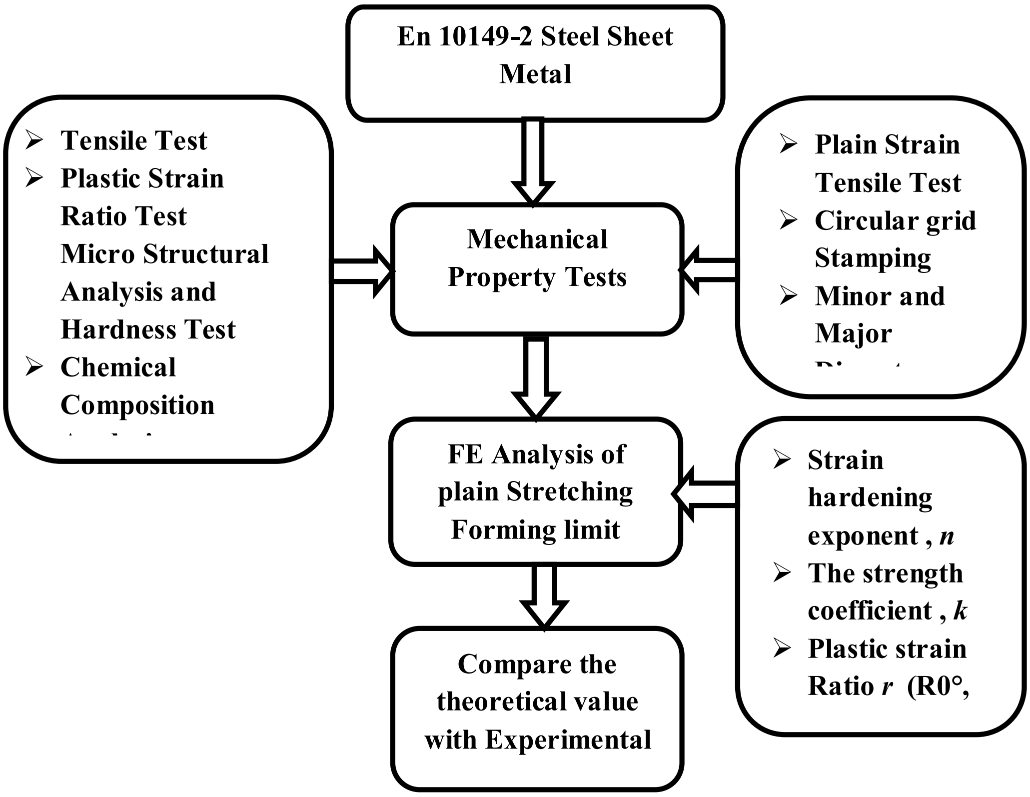

Figure 3.1 General follow diagram of sheet metal formability evaluation

3.3. Materials

EN-10149-2 steel sheet of 2.42mm thickness was used as base materials for the present work which was used in a wide-ranging of applications and economic considerations in the industries. This grade was also represented as ASTM A514 standard. Initially, the chemical composition testing was performed to know the exact elements existed in the sheets metal. Table 3.1 shows the chemical composition of selected material at room temperature.

3.3.1. Chemical Composition

Table 3. 1 EN-10149-2 alloy steel grade Chemical Composition

Element	Content	Max Value
C	0.064%	0.12 Max
Si	0.044%	0.6 Max
Mn	1.46%	2.1 Max
P	0.003%	0.025 Max
S	0.002%	0.015 Max
Cr	0.006%	Not specified
Mo	0.02%	0.5 Max
Ni	0.028%	Not specified
Cu	0.0091%	Not specified
W	0.04%	Not specified
Al	0.045%	0.15 Max
Nb	0.03%	0.09 Mxa
Ti	0.0950%	0.22 Max
Fe	98.1529%	Balance

3.4. Methodology

For this study different methodologies applied in order to evaluate the forming limit strain EN-10492-2 steel sheet of experimentally and practically. Microstructure and hardness testing experimental set up, tensile and plain stretching experimental set up also included in this chapter.

3.4.1. Microstructure Studies Procedure

The microstructure of the specimen was observed by using Metallurgical Microscope of model: Huvitz HR-300 series, magnification: 50X, 100X, 200X, 500X, 1000X, scanning area: 104x102mm, illumination system: 12v, 1000W halogen lamp (Fig. 3.2). Firstly, samples were cut from the sheet metal. Then, these specimens were mounted in phenolic resins by hot mounting press machine at Material Engineering lab, ASTU, Ethiopia (Fig. 3.3). The machine has upper ram, lower ram, cylinder, heating chamber, cooling process and mold parts. The system operates automatic mounting press that applied pressure, heat and cooling water. After that grinding with silicon carbide paper with grid size of 400, 800, 1200 and 2000 respectively and polished by using high performance diamond suspension on rotating polishing machine as shown in Fig 3.4. Finally, after proper polishing the samples were immersed in to the Keller's etchant solution formulated shown it Table 3.1 for 15 seconds. All, samples are seen at 1000x magnification for this thesis study. For that testing, specimen was prepared in rolling direction

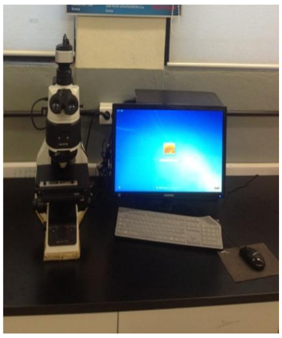

Figure 3. 2 Metallurgical Microscope

Figure 3. 3 Mounting press machine

Figure 3.4 Rotating silicon carbide paper with diamond suspension

Table 3. 2Keller's etchant used for microstructure observation

Keller's etchant	Concentration	Condition
Methanol	25 ml	15 seconds
Hydro-chloric acid	25 ml	
Nitric acid	25 ml	
Hydrofluoric acid	1 drop	

3.4.2. Hardness tests

Hardness is the resistance of a material to deformation, indentation or scratching. The basic goal of hardness testing is to quantify the resistance of a material to plastic deformation. The indentation value has high importance for technical applications which reflects the resistance to deformation which is a complex property and related to modulus, strength, elasticity, plasticity and others.

For testing hardness of the high strength steel it recommended to use either Rockwell hardness or Vickers hardness testing machine. Therefore, Vickers hardness machine is available so that in this study the sample was tested by Vickers hardness tester machine. Vickers hardness test was conducted to check the ductility of the. The Vickers hardness test used a square-based pyramid diamond indenter with an angle of 136° between the opposite face at the vertex, which was pressed in to the surface of the test piece using 10 kg forces. There were five trials performed for the samples and the average hardness (HV) was taken.

$$HV = (Constant\ x\ Test\ Force)/(Surface\ Area\ of\ Indentation)$$

$$HV = \frac{0.102 * 2F \frac{\sin 136^{\circ}}{2}}{d^2} ------------------ 3.1$$

Where: - F = force applied on the specimen

d = the diagonal distance of the indenter

3.4.3. Tensile Test Procedure

The tensile test was widely used for the measurement of basic mechanical properties of metals, plastics, and composite materials. Mechanical properties are an important measure in order to know the material properties, and the tensile test is just one way to certify the material. In tensile test, the materials properties such as elastic deformation properties (Young"s modulus and Poisson"s ratio), yield strength, ultimate tensile strength, ductile properties (elongation and reduction in area) and strain hardening characteristics.

3.4.3.1.Tensile specimen preparation

Based on the ASTM standard, there were three types of the specimens for the tensile test process where it was plate, sheet and round type specimen. In this project, sheet metal was performed to get the material properties. For this purpose, there nine (three specimen per each rolling direction) specimens were prepared from2.42mm thick EN - 10492-2 steel sheet metalcut at 0°,45° and 90° to the rolling direction of the specimens by using sheering press machine with the dimension of 200x25x2.42mm. To evaluate the mechanical properties ofthe specimen, tensile tests were performed according to the ASTM standard E-8M. This specimen was prepared from strips by using milling machine. The detail dimension and specification of the tensile test specimen prepared was shown in the Figure 3.5 and Table 3.3. The prepared specimens were as shown in Fig. 3.6 as per the standards.

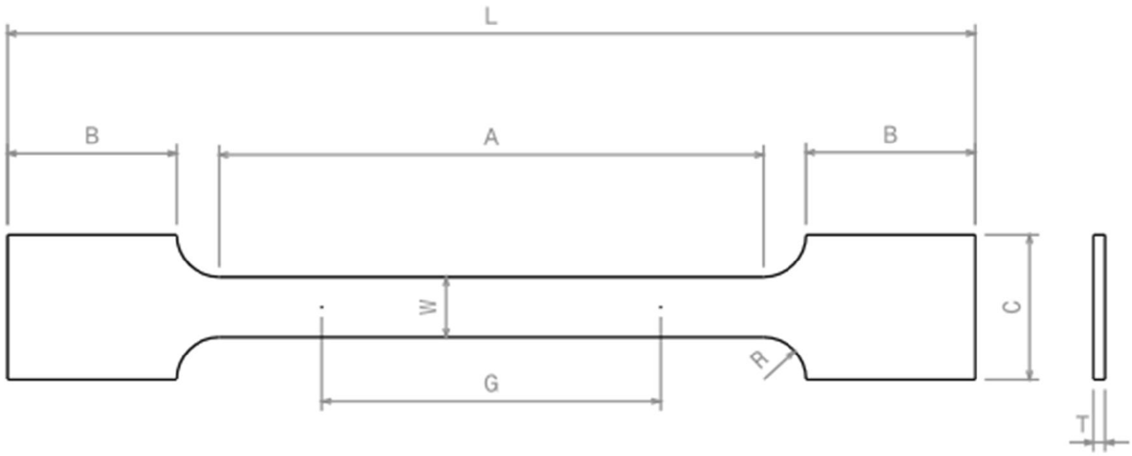

Figure 3.5 ASTM E 8/E- 8M - 08 Standard Rectangular Tension Test Specimens Dimensions

Table 3. 3ASTM E 8/E- 8M - 08 tensile test specimen Standard dimensions [40]

Dimensions	mm
G - Gauge length	50 ± 0.1
W - Width	12.5 ± 0.20
T - Thickness	2.42
R - Radius	12.5
A - Length of cross-section,	75
B - Length of grip section,	30
C - Width of grip section,	25
L – Over all Length	200

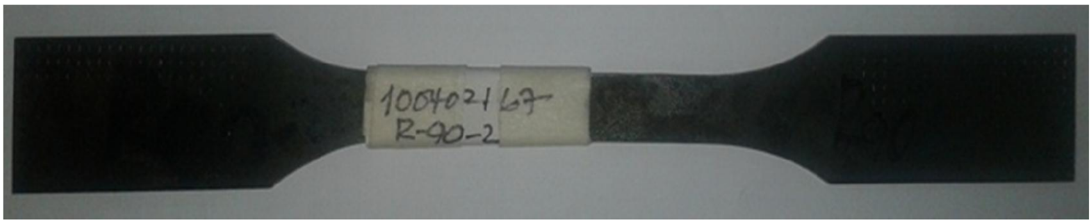

Figure 3.6 specimens prepared for tensile tests

3.4.3.2. Experimental setup for Tensile Test

The specimens for tensile tests were tested by universal testing machine (ISO 68982-1UTM 2000kN) in Ethiopian conformity assessment enterprise. The specimens held by top and bottom griper attached to universal testing machine shown in the Fig 3.5. The piston speed of the machine was automatically adjusted with the dimensions of the specimens. During the tension test, the grips were moved apart at constant rate to pull and stretch the specimen. The force on the specimen and its displacement was continuously monitored and plotted on a stress strain curve until fracture. The measurements, tensile strength, yield strength, and ductility were calculated after the tensile test specimen broken.

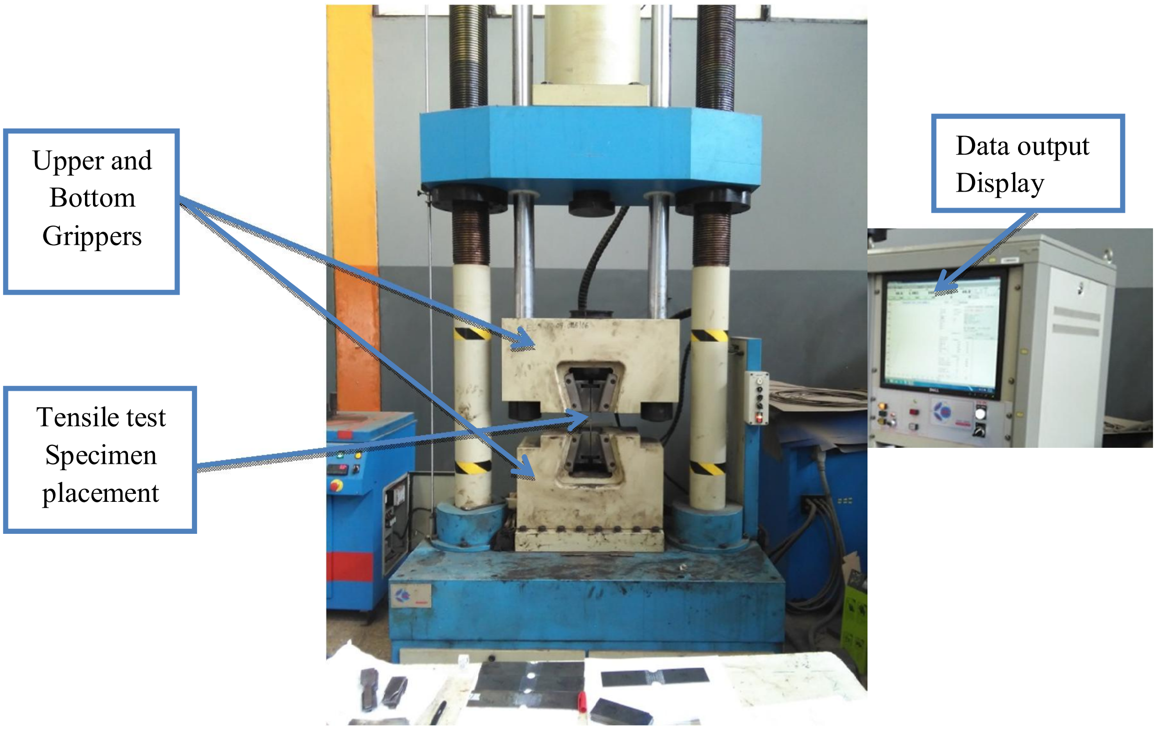

Figure 3. 7 ISO 68982-1 uniaxial tensile testing machine

3.4.4. Plane-Strain Tension Testing

Plane-strain stretching is an important type of deformation because most materials fracture at a lower level of strain in plane strain than in any other condition. Plane-strain stretching results in elongation in one direction and no dimensional change in the perpendicular direction. The test does not provide information on the response of sheet materials in the plane-strain state, in which the minor strain is zero. However, it can be modified to produce this strain state in part of the sample. These are wide sample method or widths constrain method. [41]

3.4.4.1.Wide Sample Method

Increasing the width of the sample and decreasing the gage length changes the strain state from one with a large negative minor strain component toward the plane-strain state, in which the minor strain component is zero. In the rectangular sheet tension test, samples with length-to-width ratios of 1 to 1, 1 to 2 and 1 to 4 are used to approach the plane-strain conditions [42]. Gage lengths are constrained further by reinforcements welded onto each side of the sample at both ends, thus making the samples three layers thick except in the gage length.

3.4.4.2.Width Constraint Method

In this method, a rectangular sample is used that has a central gage section reduced in width by circular notches [43]. The gage section is clamped between two pairs of opposing parallel knife edges (stingers) aligned with the sample axis. The knife edges prevent transverse (width) strain in this region. The sample is pulled to fracture in a tension-testing machine, and the plane-strain limit (necking) and fracture strains are determined from thickness measurements made on the fractured sample. The use of a spring-loaded clamp around the knife edges makes adjustment of the clamp during testing unnecessary.

3.4.4.3. Plane-Strain Tension Test sample preparation

In this project, sample prepared based on the width constraints method. The dimension of the specimen is as shown in Fig. 3.8. For this purpose, there nine (three specimen per each rolling direction) specimens were prepared from2.42mm thick EN - 10492-2 steel sheet metal cut at 0°,45° and 90° to the rolling direction of the specimens by using sheering press machine with the dimension of 300x40x2.42mm. This specimen was prepared from strips by using milling machine Fig 3.9.

3.4.5. Experiment set up for Plain stretching test

For the Plane strain tensile test same like uniaxial tensile test performed by universal testing machine (ISO 68982-1UTM 2000kN) in Ethiopian conformity assessment enterprise. The specimens held by top and bottom griper attached to universal testing machine shown in the Fig 3.10.During the tensile test, the grips were moved apart at constant rate to pull and stretch the specimen. The force on the specimen and its displacement was continuously monitored and plotted on a stress strain curve until fracture and the parameter measured from the tested specimens are minor and major diameters of the circular grids after deformation or fractured.

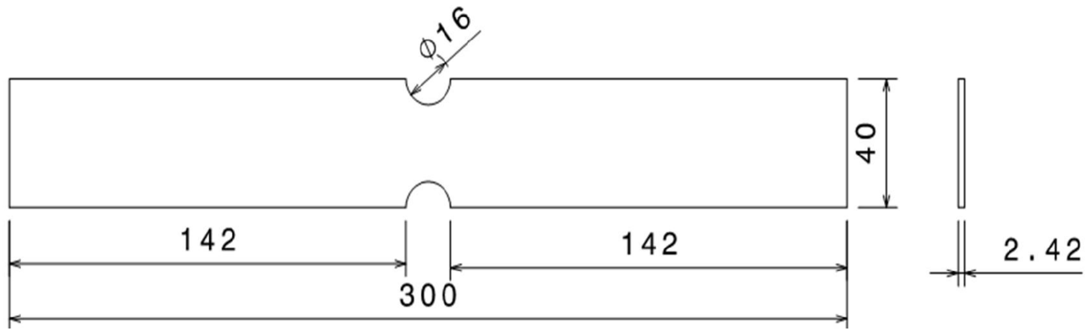

Figure 3. 8 Dimension for Plane- strain tension test

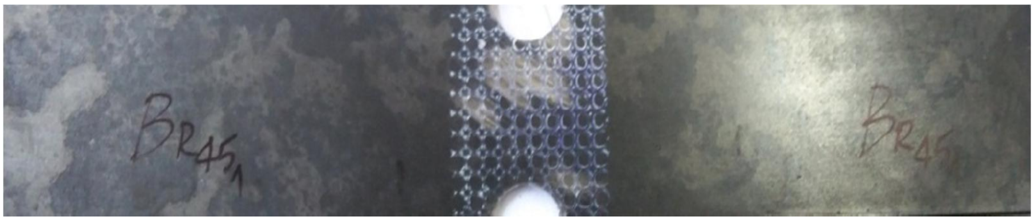

Figure 3.9 Typical Plane - strain tension specimen before test

Figure 3.10 Experimental set up for Plane Strain tension tensile test

3.4.6. Grid marking and strain analysis

Grid marking is one of the commonly used strain measurement methods for strain analysis in sheet metal forming processes due to the relative simplicity [44]. It consists of a very small diameter circle or square grid pattern (approximately a range from 1 to 8 mm) [45]. Grid marking is the process of printing line patterns in the area of interest on the sheet metal blank [46]. The most widely used method or measuring deformation is to mark the sheet by etching or scribing or by means of ink, dye, or paint and to measure the changes in the separations of the marks caused by the deformation.The utilized grid pattern should be very precise in order to obtain accurate results from the strain analysis [47]. Strain analysis by grid marking is a practical method, which has been utilized effectively to solve problems in metal forming [48]. For grid marking measurement different measuring techniques are used. These include both manual and automated measurement methods.

In this study the circular grid prepared by the rubber stamping materials with circular diameter of 3.0mm as shown in Fig 3.11. The marking process was done by using paint as shown in the Fig 3.12.

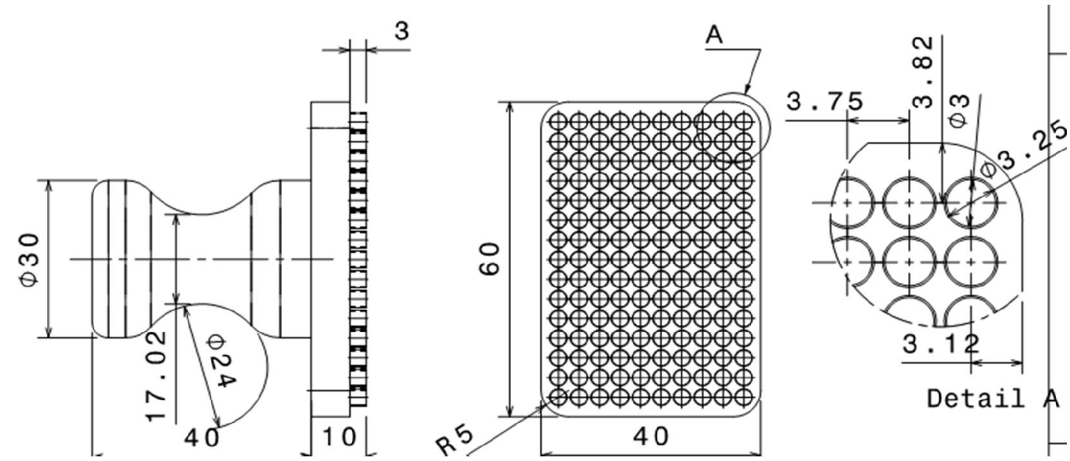

Figure 3. 11 Circular grid stamp dimension

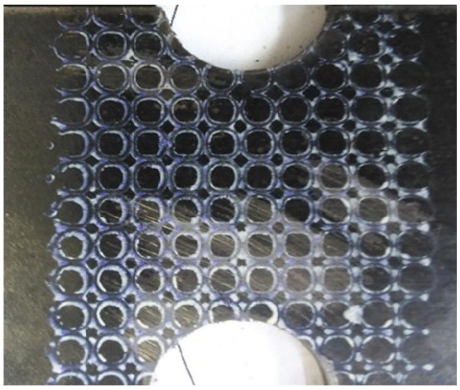

Figure 3. 12circular grids marking on the specimen

3.4.7. Plastic Anisotropy Test

In tensile stress testing, the value of plastic strain ratio is associated with gradient of corresponding component strain plot. When the plot of strain is linear the value of plastic strain is constant, so that in the ratio, total plastic strains may replace incremental strain.

3.4.7.1. Sample prepared for plastic anisotropy Test

In this study sample prepared base on the ASTM-E517 standard specimen dimension used for the test of plastic strain ratio is shown in Fig 3.13. The dimensions of the specimens are listed in Table 3.6. The specimens are prepared by cutting three different orientations from 2.42mm thickness of EN - 10492-2 steel sheet metal in the orientation of rolling direction(RD) 0°, transvers direction (TD) 90° and diagonal direction (DD) 45°. In plastic strain ratio test, the length and width of the specimen are not critical. But, special care was taken to stretch the gage section in uniform manner to avoid griper effects and anomalous change along gauge length.

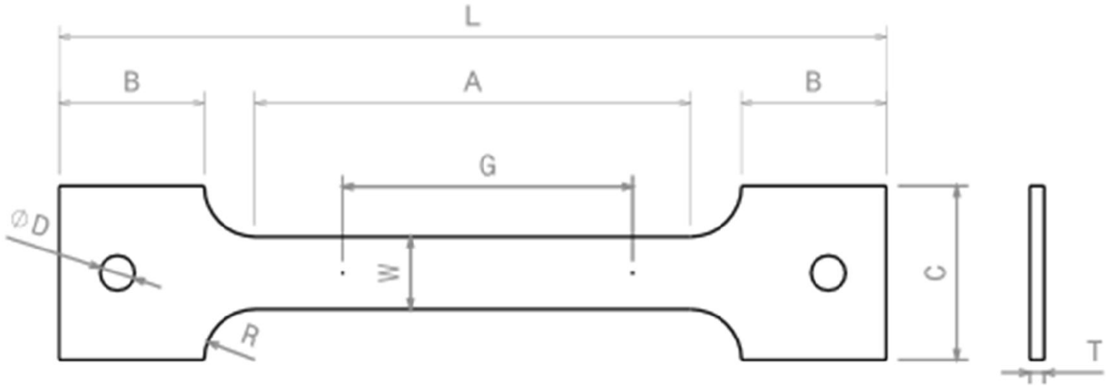

Figure 3. 13 ASTM-E517 standard dimension specimens for plastic strain ratio test

Table 3. 4ASTM-E517 standard Dimension specimens for plastic strain ratio test

Dimensions	mm
G - Gauge length	50 ± 0.1
W - Width	12.5 ± 0.20
T - Thickness	2.42
R - Radius	12.5
A - Length of cross-section,	75
B - Length of grip section,	50
C - Width of grip section,	25
L – Over all Length	142

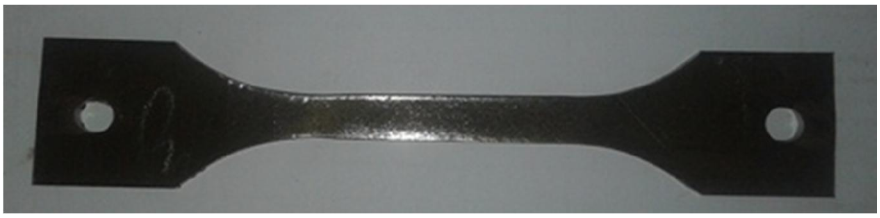

Figure 3. 14 Typical Specimen for plastic strain ratio test

3.4.8. Experiment Procedure of Plastic Strain test

- The original width of the specimen, w_o is marked to dimension of 2.42 mm at the mid-point of the specimen.
- The original length of the specimen, l_o is marked to dimension of 2.42mm at the mid-point of the specimen
- The specimen pulled axially until 2% elongation, and then the process was stopped.
- The final width w_f, and gauge length lf, is measured in similar manner to initial measurements.

3.4.9. Simulation details

Finite element method was used for numerical analysis of sheet metal forming operations. The numerical analysis of formability evaluation was done by PAM STAMP- 2G software. CAD models of the specimens were generated with same dimension of experiment by using CATIA V5 R20® software as shown in Fig. 2.15 and imported into PAM-STAMP2G®, an elasto-plastic finite element code for preprocessing, solving and post-processing.

These CAD models were meshed using Deltamesh facility in PAM-STAMP 2G®. The meshing was done with quadrilateral shell elements of the Belytschko–Tsay formulation, with five through-thickness integration points. The average mesh size of about 1 mm was kept throughout the specimen with number elements of 4586.Simulationswereperformedfor same geometries of the blank to develop complete strain-path limits using appropriate boundary conditions. These conditions are one end of the model is fixed and the other end is free.

The base material properties and parameters used of EN-10149-2 Sheet metal is given in Tables 3.7were incorporated during simulations.

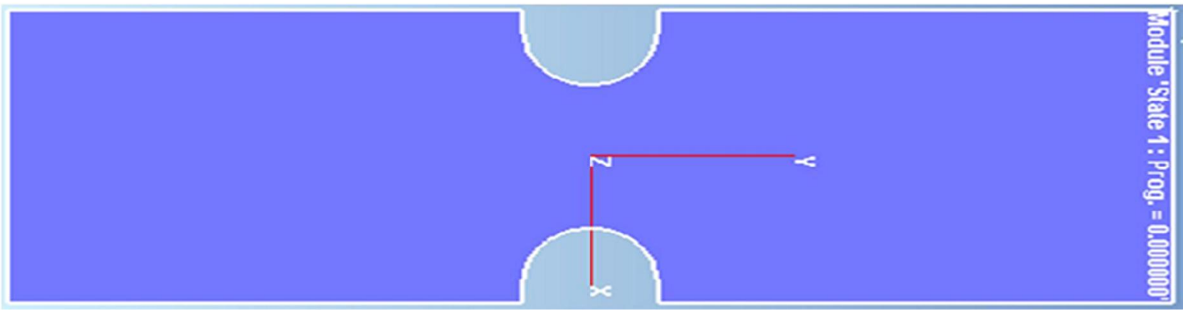

Figure 3. 15CAD model of the specimen

Table 3. 5 Simulation Parameters

Parameters	Expression
Thickness of sheet	t
Rolling direction (R)	R_0, R_{45}, R_{90}
Modulus Elasticity	E
Passion ratio	γ
Density	ρ
Plasticity Law	Hill's 48
Anisotropy Type	Orthotropic
Hardening Curve	Holloman's law

CHAPTER FOUR

4. RESULTS AND DISCUSSIONS

This chapter discusses the tensile test result, data analysis, the microstructure result, hardness testing and plane stretching test results that were obtained by the testing method described in previous chapter. It presents the forming limit strains that were calculated using the Keeler-Brazier equation. This chapter also provides a comparison of forming limit diagram results that have been calculated from the forming limit strain data collected in the current study to strain data converted to PAMSTAMP - 2G software.

4.1. Uniaxial Tensile Test

In tensile test, sample was typically pulled to its breaking point to determine the ultimate tensile strength of the sheet. The amount of load applied to the specimen and the elongation of the specimen were measured throughout the testing process. The properties of materials were expressed in terms of stress, which is the ratio of applied force to the area and strain, which was the percent change in length. To obtain the result of stress during the test, the force measurements were divided by the sample's cross-section area as shown in equation 4.1 and the value of strain is also obtained from equation 4.2 [40], by dividing change in length to the original length of the specimen. Both the value of stress and strain presented on x-y plot or stress-strain curve.

$$\sigma = \frac{F}{A} \text{-----------------------------} 4.1$$

$$\varepsilon = \frac{\Delta L}{L} \text{-----------------------------} 4.2$$

4.1.1. Stress-strain relationship

During tensile test, the dimensions of the specimen changes with the deformation process, hence true quantity are better indicator of the engineering quantities. The engineering quantities of train and stress are depending on the original dimensions of the sample. From tensile test, the value of the progress of load, change in length per time and change in cross-section was used to calculate the engineering strain and stress. The original length, $L_{0,}$ is taken from original gauge length from the standard sample. The equation for engineering strain, e, and Engineering stress are based on the nominal change in length(ΔL), force and nominal cross section area is given:-

$$e = \frac{\Delta L}{L} ------------------------ 4.3$$

$$S = \frac{F}{A_0} ------------------------ 4.4$$

Where:-

e = Engineering Strain, F = Applied Force

S = Engineering Stress, A_0 = Initial cress section

ΔL = change in length, L_0 = original gage length

The true strain and stress are not depending on the original length and diameter;

$$\varepsilon = \ln(1 + e) ------------------------ 4.5$$

$$\sigma = S(1 + e) ------------------------ 4.6$$

Where:- ε = True Strain, σ = True stress

4.1.2. Strain-hardening exponent (n value)

The strain hardening exponent is equal to the slope of the true stress/true strain curve up to maximum load, when plotted on log-log coordinates. The n-value relates to the ability of a sheet of material to be stretched in metalworking operations. Hollomon equation describes the strain hardening behavior of sheet metal deformation. It is given by:

$$\sigma = K\varepsilon^{n} ----------------------4.7\ [49]$$

Where, σ is the true stress, ε is the true strain, and K, the material strength coefficient,

The value n in eq. 4.7 relationship is equal to the true stress at a true strain of 1.0. The higher the n-value means the better the formability (stretch ability) of the material. It is also known as the strain-hardening coefficient.

The strain hardening exponent ‘n’ is used to measure the amount of strain hardening. It is a constant value calculated from the slope of natural logarithmic value of true strain-true stress graph. The natural logarithmic value of true strain and true stress was selected from the value in between yield strength and ultimate tensile strength. To plot the graph between $\ln(\sigma)$and$\ln(\varepsilon)$, the equation,$\ln\sigma = \ln k + n\ln\varepsilon$, used in the same way of the equation of line: $Y = C + mX$

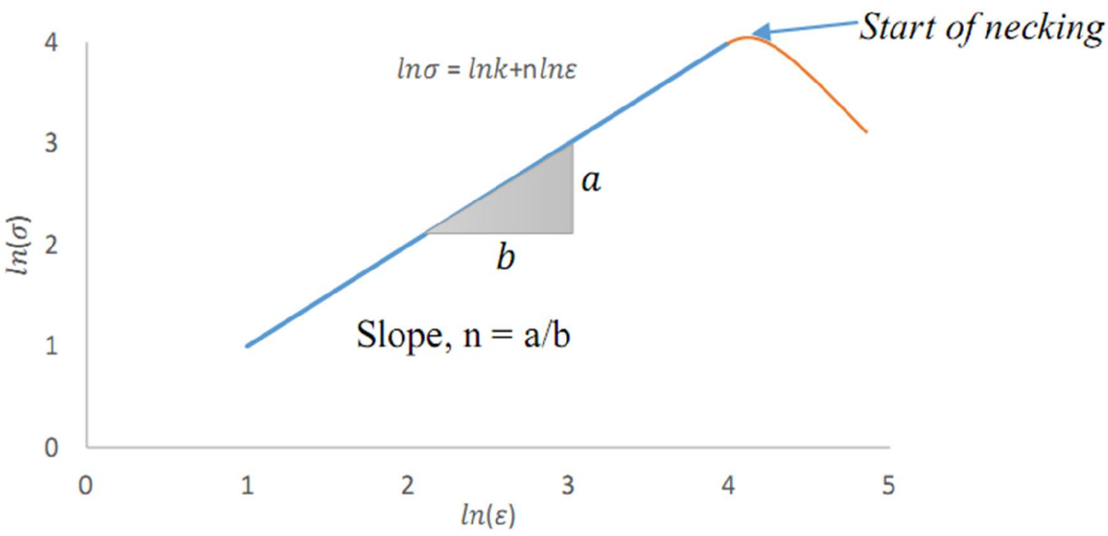

Figure 4.3 Schematic graph of Natural logarithmic of true stress-train

4.1.3. Hill's 48 yield criterion

A well-known quadratic anisotropic yield criterion proposed by Hill is one of the most widely used yield functions and which was an extension of Von-Mises criterion. The Hill's 48 yield model assumes that a material exhibits three mutually orthogonal planes of symmetry. The principal axes of anisotropy are denoted as x, y and z, about which the material properties have twofold symmetry [50]. This yield function has been successfully applied for modeling various kinds of steel sheets. This criterion has validated the plastic potential of many common materials which undergo uniform deformation in all directions. The Hills Yield criterion used to determine the initial yield surface and the equivalent plastic strain. In his equation, Hill considers tensile stress and compressive stress at the same yield stress and the homogenous quadratic with no single shear stress occurs linearly. Also there is no hydrostatic pressure effect on yielding. Hence, the plastic potential assuming the orthogonal principle axes as reference takes the form. TheyieldpotentialoftheHill's48yield criterion is representedby:

$$2f(\sigma) = F(\sigma_{yy} - \sigma_{zz})^2 + G(\sigma_{zz} - \sigma_{xx})^2 + H(\sigma_{xx} - \sigma_{yy})^2 + 2\left(L\sigma^2{}_{yz} + M\sigma^2{}_{zx} + N\sigma^2{}_{xy}\right) = 1 ----------- 4.8$$

Under plane stress condition, $\sigma_{zz} = \sigma_{yz} = \sigma_{zx} = 0$. Therefore, the above equation can be written as:-

$$2f(\sigma) = (F+H)\sigma_{yy}{}^2 + (G+H)\sigma_{xx}{}^2 - 2H\sigma_{xx}\sigma_{yy} + 2N\sigma^2{}_{xy} = 1 ------ 4.9$$

Where:- σ_{xx} = normal stresses in the rolling

σ_{yy} = normal stresses in the transverse and

σ_{zz} = normal stresses in the thickness direction

$\sigma_{xy} = \sigma_{yz} = \sigma_{zx}$, are the shear stresses in xy, yz and zx plane, respectively. F, G, H and N are the anisotropic coefficients parameters. If the parameters F, G and H are equal to 1 and N has the value of 3, the Hill's 48 yield model will be reduced to the von-Misses model. The material parameters of the Hill's 48 yield model is principally obtained by determination of the r values along 0°, 90° and 45° to the rolling direction. From Eq. (4.9), the anisotropic parameters F, G, H and N can be formulated in terms of the r values r_0, r_{45}, and r_{90} as followed:

$$F = \frac{r_0}{r_{90}(1 + r_{90})} ------------------------ 4.10$$

$$G = \frac{1}{(1 + r_0)} -------------------------- 4.11$$

$$H = \frac{r_0}{(1 + r_0)} -------------------------- 4.12$$

$$N = \frac{(r_0 + r_{90})(1 + 2r_{45})}{2r_{90}(1 + r_0)} --------------------- 4.13$$

Uniaxial tensile tests of samples prepared from different directionswere performed to characterize the r-values and the yield stress in the rolling direction.

4.2. Anisotropy Coefficient

The characteristics of the rolling process and due to their crystallographic structure, sheet metals generally exhibit a significant anisotropy of mechanical properties. The formability of sheet metal depends upon the resistance of thinning or thickening. The plastic strain ratio is useful for evaluating materials selected for forming different shapes geometries. Lankford parameter or the anisotropy coefficient (plastic strain ratio) is the variation of sheet metal plastic behavior with rolling direction.[51]. It can be defining also the parameter that shows the ability of sheet metal to resist the thinning or thickening. This coefficient is determined by uniaxial tensile tests on sheet specimens in the form of a strip. And plastic strain ratio, the specimen pulled between gripers to the length direction and change in gauge length and thickness is recorded. The anisotropy coefficient (r) is defined the ratio of true width strain to true thickness strain.

$$r = \frac{\varepsilon_w}{\varepsilon_t} ------------------------- 4.14$$

Where, ε_w and ε_t are the strain in width and thickness direction, respectively. Eq. 4.14 can be written in the form ε_w and ε_t .

$$r = \frac{\ln \frac{b}{b_0}}{\ln \frac{t}{t_0}} ------------------------- 4.15$$

Where b_o and b are the initial and final width, while t_o and t are the initial and final thickness of the specimen, respectively.

Taking into account the condition of volume constancy Therefore the above relationships are replaced by one implying quantities having the same order of magnitude: length and width of the specimen.

$$\varepsilon_w + \varepsilon_t + \varepsilon_l = 0 ---------------------- 4.16$$

Eq. 4.16 becomes

$$r = -\frac{\varepsilon_w}{\varepsilon_t + \varepsilon_l} ----------------------- 4.17$$

Eq. 4.16 becomes

$$r = \frac{-\ln \frac{b}{b_0}}{\ln \frac{l}{l_0} + \ln \frac{b}{b_0}} ----------------------- 4.18$$

Where l_o and 1 are the initial and final gage length.

Eq. 4.18 can be rearranged as follows.

$$r = \frac{\ln \frac{b}{b_0}}{\ln \frac{l_0 . b_0}{l . b}} ----------------------- 4.19$$

This relationship is used in practice for evaluating the anisotropy coefficient. By convention the r - values usually are determined at 20% elongation for the purpose of comparison. Modem tensile testing machines perform instantaneous measurement of the quantities required for evaluating the anisotropy coefficient and calculate it during the test. Values of r at 20% elongation as well as its variation with strain can be determined [52].

4.2.1. Tensile Test Results and discussions

The fig 4.1 and 4.2 show the material EN-10149-2 sheet metal steel uniaxial tensile test specimen before and after the testing respectively. Fig. 4.2 shows the tested specimen at different rolling direction (RD) 0°, 45° and 90°. As shown in the figure the fracture line direction is more or less coincide to the rolling direction. Hence, for rolling direction (0°) the fracture line has some inclined angle, for diagonal direction (45°) the fracture line makes parallel to the orientation and for the transverse direction (90°) the fracture line makes perpendicular to the orientation.

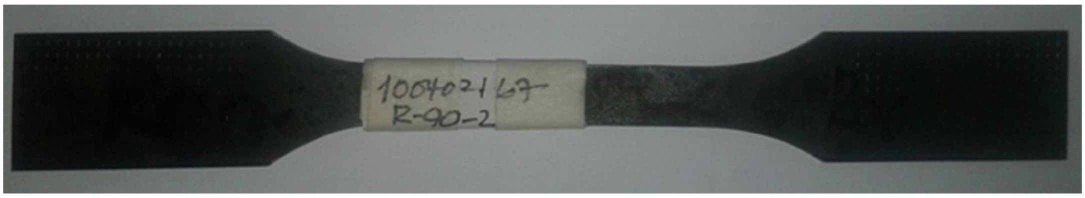

Figure 4.2EN-10149-2 steel sheet metal Specimen before Tensile Test

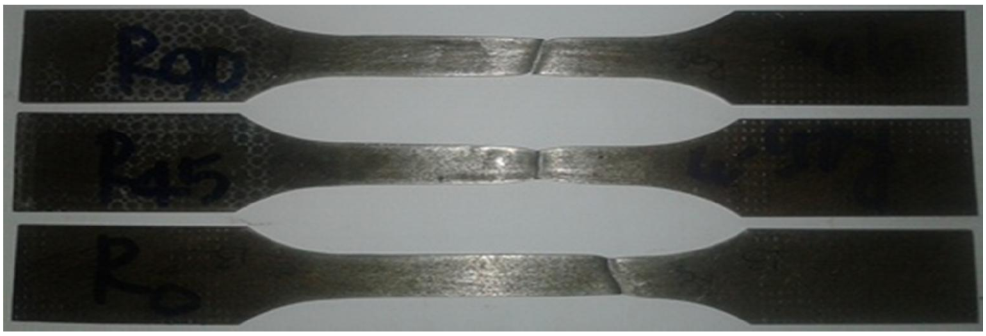

Figure 4.3EN-10149-2 steel sheet metal Specimen after Tensile Test

The mechanical properties of the EN-10149-2 sheet metal found from the uniaxial tensile tests result are given in the Table 4.1.These are yield stress, uniform elongation, tensile stress, material strength coefficient (*K*) and strain hardening coefficient (*n*). The yielding stress and tensile strength for rolling direction specimens is the highest when it is compared with the result from others RD specimen as presented in Table 4.1 and 4.2.

The base material engineering stress-strain behavior at different rolling directions is shown in Fig. 4.3. Table 4.1 shows the tensile properties of all three reputations and Table 4.2 summarizes the mechanical properties of EN-10149-2 base material obtained in the present work. The yield strength and ultimate tensile strength are found to be within 972-1020 MPa and 1018-1054 MPa respectively. The uniform elongation and strain hardening exponent are about 6.8% and 0.22 respectively in all the rolling directions.

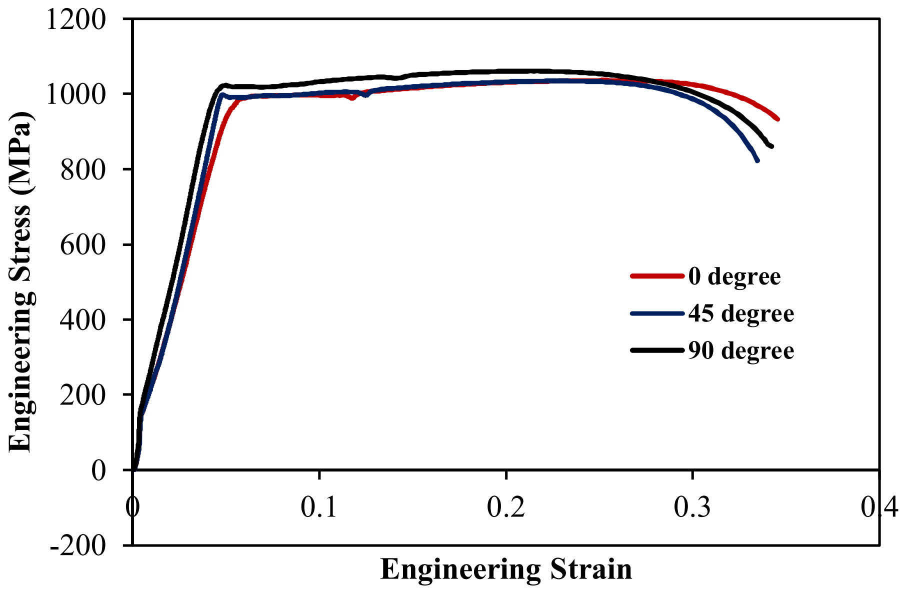

Figure 4.4 Tensile behavior of EN - 10492-2 steel sheet metal in different rolling directions

Table 4.3indicates summarized mechanical properties of EN-10149-2 sheet steel and same used for simulation of Plane stretch formability. The mechanical properties and anisotropy value shown in Table 4.3 are the average experimental values obtained from tensile test and plastic strain ratio test. The highest anisotropy value (R = 1.287) observed at the 45° rolling direction which implies at this direction there is a higher tolerance or dalliance of fracture which helps more forming strain attains. The higher R value indicates highest forming limits.

Table 4. 1 Tensile Test Results of EN-10149-2 sheet metal

Rolling Direction	Trial	YS (MPa)	Uniform Elongation (%)	Tensile Strength (MPa)	Material Strength Coff (K) (MPa)	Strain Hardening Exponent (n)
0°	1	951.5	5.4	999.3	1512.6	0.142
	2	997.2	7.6	1021.3	1744.5	0.211
	3	983.0	7.6	1036.1	1763.6	0.209
45°	1	927.1	5.2	973.8	1425.7	0.126
	2	968.3	8.2	1023.6	1776.1	0.222
	3	1020.7	6.5	1060.9	1603.1	0.1436
90°	1	1058.8	6.8	1090.5	1628.7	0.1378
	2	1009.2	6.8	1039.62	1796.1	0.215
	3	994.3	6.9	1034.6	1676.1	0.1804

Table 4. 2 Average Resultsof mechanical property of EN-10149-2 (S700mc) sheet metal material

Rolling Direction	YS (MPa)	Uniform Elongation (%)	Tensile Strength (MPa)	Material Strength Cof (K) (MPa)	Strain Hardening Exponent (n)
0°	977.3±20	6.87±10	1018.9±20	1673.6±50	0.187±0.014
45°	972.03±30	6.63±3	1018.4±31	1601.6±70	0.164±0.048
90°	1020.7±20	6.8±0.1	1054.9±40	1700.3±70	0.178±0.037

Table 4. 3 Mechanical property and Plastic Anisotropy (r - value) of EN-10149-2 (S700mc) sheet metal

Rolling Direction	YS (MPa)	Uniform Elongation (%)	Tensile Strength (MPa)	Material Strength Coff. (K) (MPa)	Strain Hardening Exponent (n)	R_0	R_{45}	R_{90}
0°	977.3±20	6.87±10	1018.9±20	1673.6±50	0.187±0.014	0.992	1.287	1.268
45°	972.03±30	6.63±3	1018.4±31	1601.6±70	0.164±0.048			
90°	1020.7±20	6.8±0.1	1054.9±40	1700.3±70	0.178±0.037			

4.3. Microstructure Result

Metallographic investigations were carried out on the sample. The sample immersed in the Keller's etchant solution for 15 seconds; this etchant was used to reveal the banded structure, and the grain boundaries and carbide containing phases. A typical microstructure of High strength low alloying presented in Figures 4.5 [52].

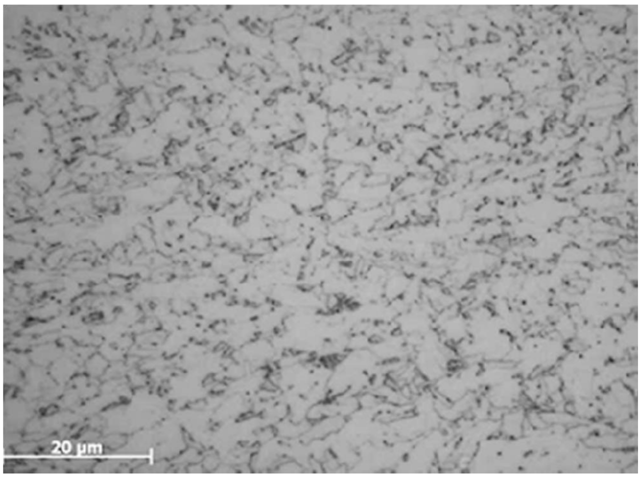

Figure 4. 5a typical HSLA steel micro structure

The grinding and polishing ofEN-10149-2 sheet steel at different steps has shown Fig.4.6.

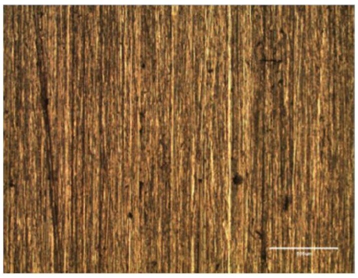

a) Grit Mesh 400CC

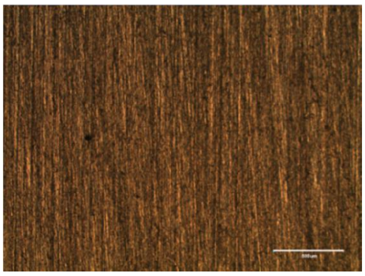

b) Grit Mesh 800CC

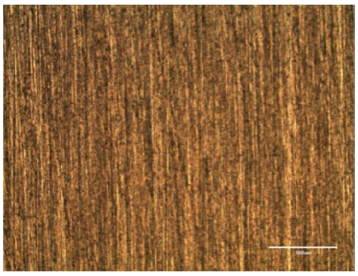

c) Grit Mesh 1200CC

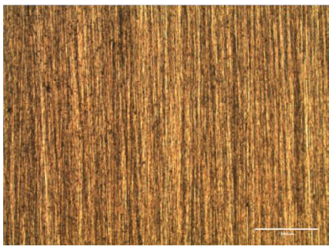

d) Grit Mesh 2000CC

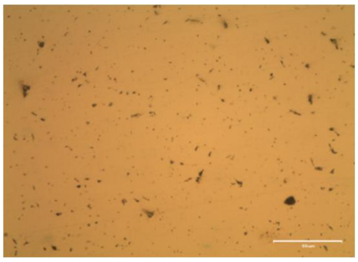

e) As Polished

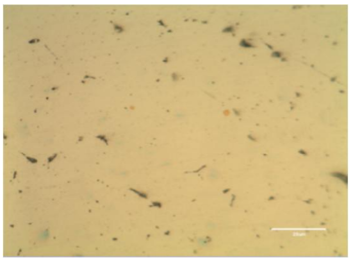

f) As Polished 1000x

Figure 4. 6Different scale of EN-10149-2 (S700mc) during grinding and polishing

In Fig 4.7 shows the microstructure of EN - 10492-2 steel sheet metal, it consists of more perlite and α-ferrite matrix microstructure with small carbide boundary. The micro structure more

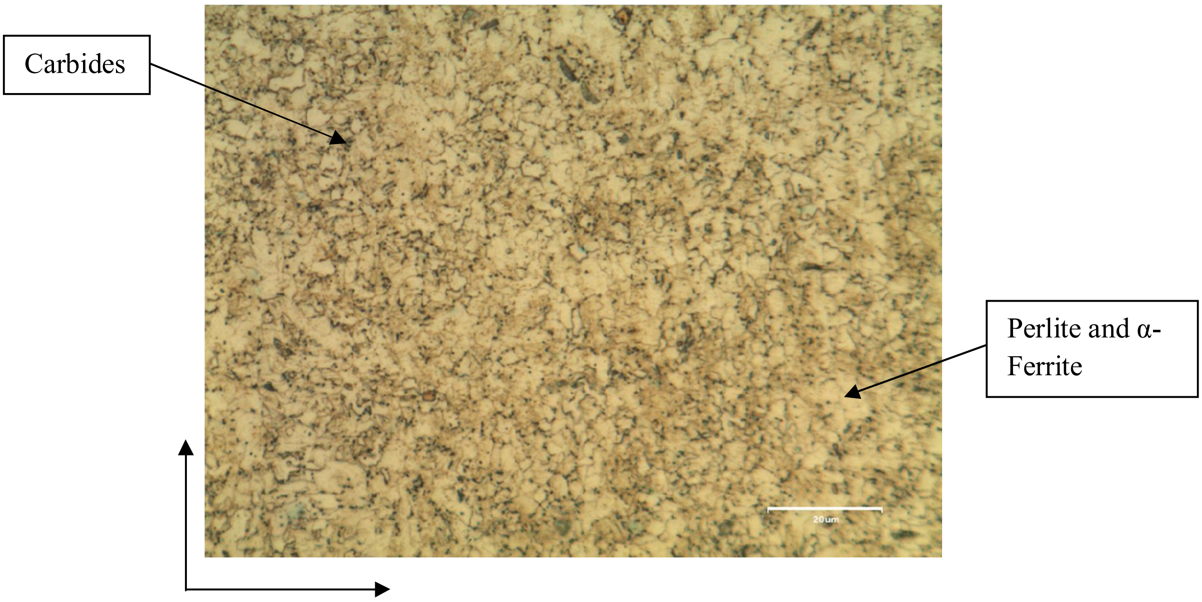

Figure 4. 7 Microstructure of EN-10149-2 (S700mc) at room temperature

4.4.Evaluation of Hardness

The microstructure image 1000X of EN - 10492-2 steel sheet metal material tested by Vickers hardness (VHR) tester, for samples there are five trials were performed with 10 kg load. Figure 4.8 indicate the surface of sample which was hardness test was performed. The average hardness number of the sample is 124.94. Tables 4.4 show the trials of test for samples.

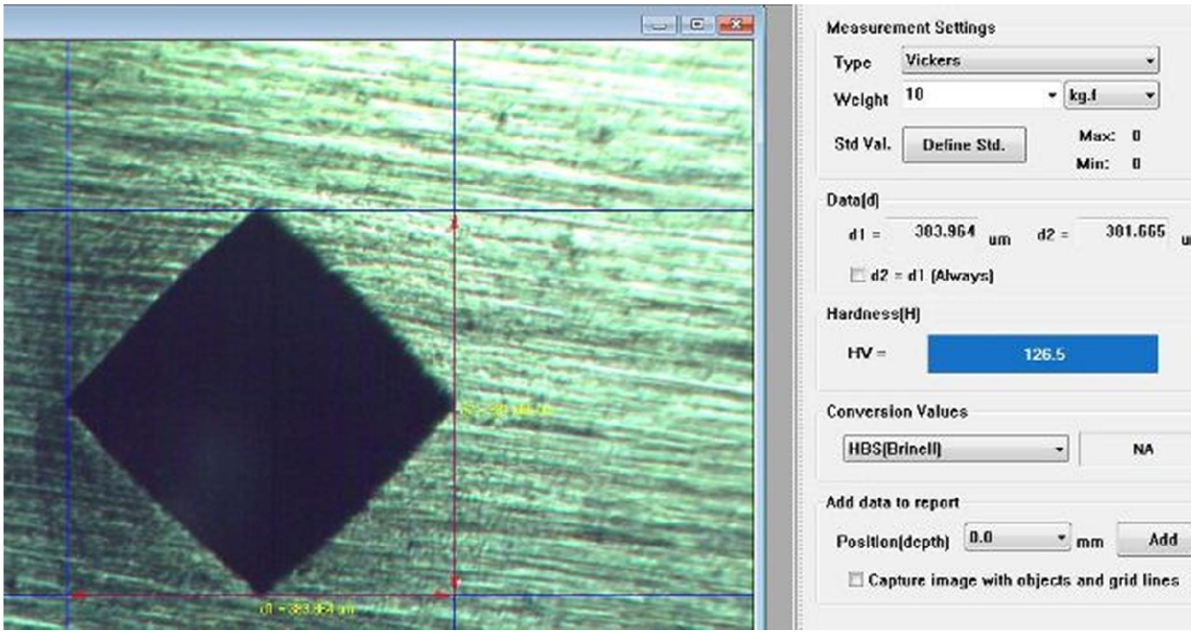

Figure 4. 8Hardness Tested of after sample

Table 4. 4 Vickers Hardness test value

Trials						
Force	HV - 1	HV – 2	HV - 3	HV - 4	HV - 5	Average
10 kgf	122.10	126.10	124.60	126.50	125.40	124.94

The average hardness number of the sample is relatively less than from mild steel and hardened steel which are 140HV and 900HV respectively. If the material has more hardness value means greater resistance to indentation and less formable. The results show that the material is formable.

4.5.In-plane plane stretching test Result

The samples prepared in three rolling direction namely, 00 (RD), 45^0 (DD) and 90^0(TD), with two test sample per rolling direction. The limit strains are evaluated by measuring the length of the major and minor axes of deformed circular grids at near the failure region of EN-10149-2 sheet blanks. Figure 4.9 and4.10showsthe method of measuring circular grids printed on the surface of base materials before and after deformation, during IPPS formability tests with photographs. The digitized caliper two digits decimal was used to measure the circular grids before and after deformation of base materials for evaluating true major and minor limit strains.

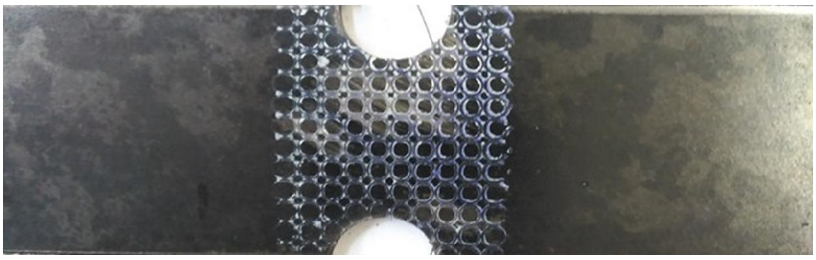

Figure 4. 9method of grid measurement before deformation

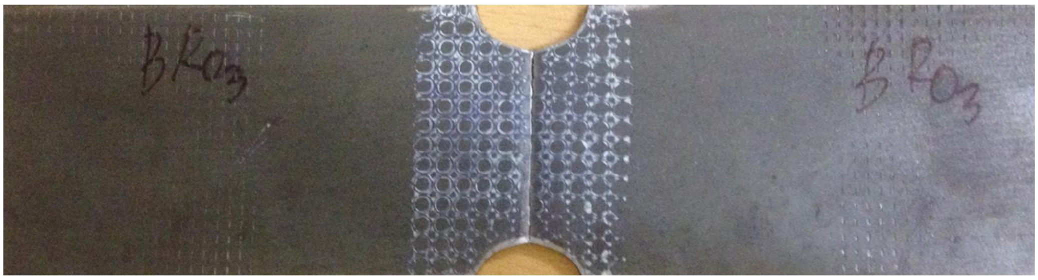

Figure 4. 10method of grid measurement after deformation

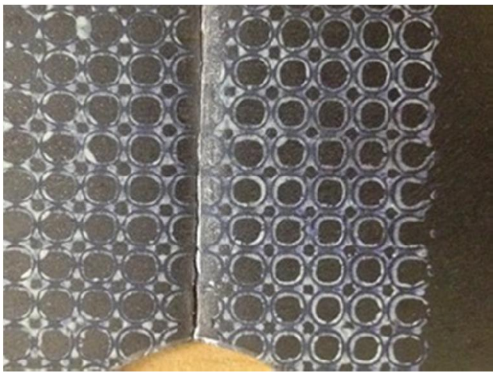

Figure 4. 4magnified Circular grid stamped deformed Sample

4.5.1. Load Vs. elongation Evaluation

In the Plane stretching test investigation as shown in the figure 4.12 the largest load applied for the transverse direction (TD) and its elongation is small relative to diagonal direction (DD). The smallest elongation and load applied occur at the rolling direction (RD). This shows the 45° rolling direction delayed for fracture this implies more formability tolerated in this direction.

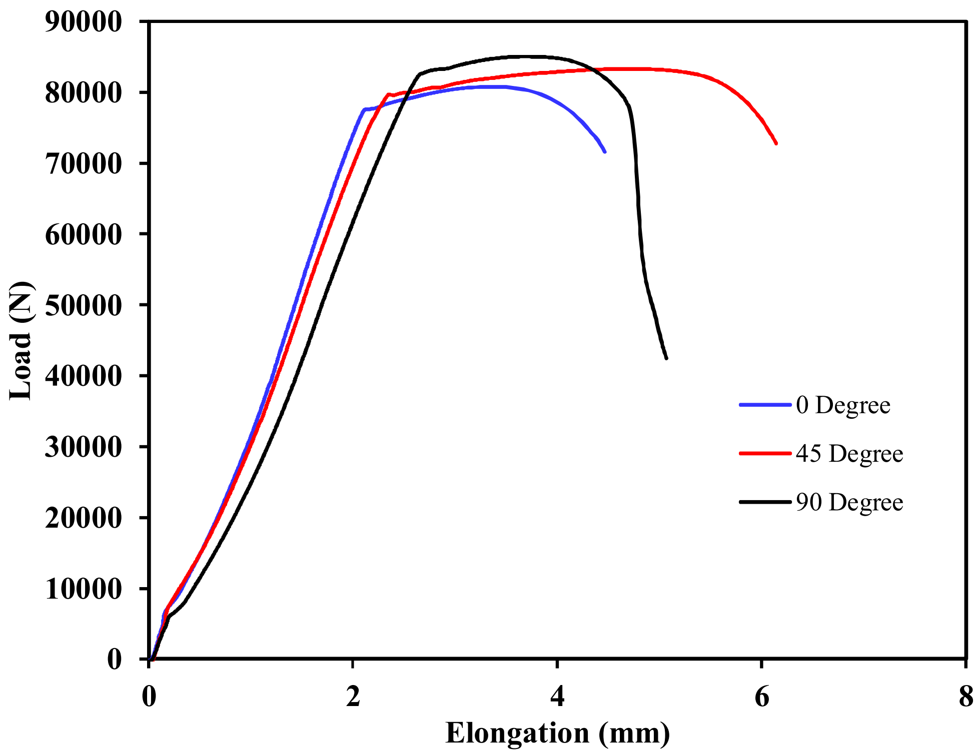

Figure 4. 5 Load to Elongation comparison

4.6. Failure criteria used for limit strains prediction

In the present experiments and simulations performed, element pairs where the thickness ratio equals or falls below 0.92 are considered as necked elements. The major strains in all the thinner elements are noted down. The maximum major strain and the corresponding minor strain of such elements are treated as the forming limit strain. This procedure of obtaining the limit strain is followed for all in-plane plane-stretching tests. Table 4.5 shows the limit strain the measured results using TGNC from in-plane plane-stretching tested samples in three different rolling directions.

Figure 4.14 shows the limit strain comparison of three (0°, 45°, 90°) different rolling direction with two reputation. The Average limit strain of each rolling direction comparison is made in Fig. 4.15. Limit strain are evaluated using the TGNC after experiment on three rolling direction. The maximum limit strain is appeared for the rolling direction of 45° and followed by the 90° and 0°. This indicates that the maximum formability is in 45° rolling direction during in-plane plane-stretching test.

Table 4. 5 Limit strains results using TGNC from in-plane plane-stretching tested

Orientations	Trials	*Measured circle diameter*	*Measured - original diameter*	$R_{thickness}$ Gradient	Major strain	Minor strain
0 degree	1	**3.124**	**0.124**	0.9193	0.124	0.104
		3.114	**0.114**			
	2	**3.231**	**0.231**	0.9166	0.252	0.114
		3.252	**0.252**			
45 degree	1	**3.572**	**0.572**	0.91783	0.57	0.541
		3.525	**0.525**			
	2	**3.424**	**0.424**	0.91973	0.464	0.192
		3.461	**0.464**			
90 degree	1	**3.451**	**0.451**	0.92011	0.451	0.353
		3.416	**0.416**			
	2	**3.294**	**0.294**	0.91588	0.321	0.264
		3.321	**0.321**			

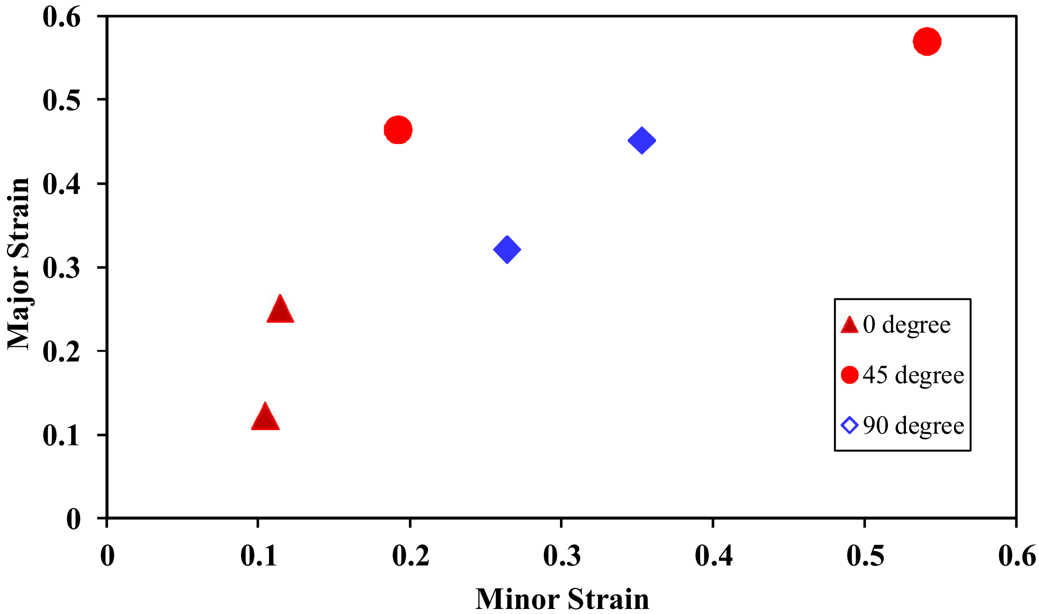

Figure 4. 6 Comparison of limit strain of in-pane plane-stretching test on three rolling directions with two reputes

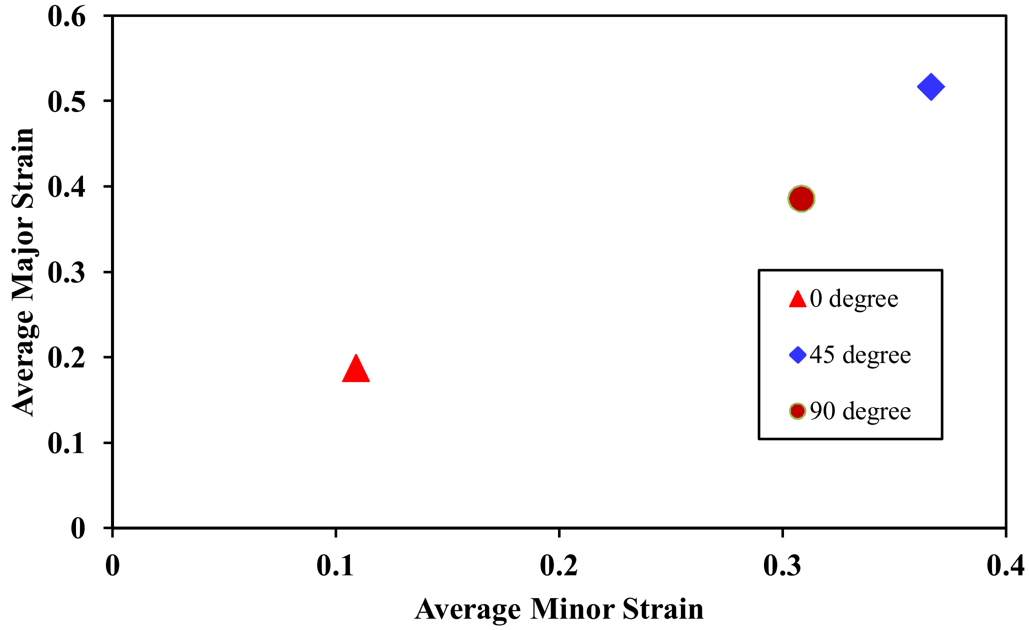

Figure 4. 7Comparison of average limit strain of in-pane plane-stretching test on three rolling directions

4.7.In-Plane Plane-stretching Simulation

Figure 4.16 shows the specimens for In-Plane Plane-stretching experiment and simulation. The specimen dimension for the simulation is followed according to the experiment specimen.The simualtion procedure is followed as mention the methodology section 3.2.13.

The simulation was performed in the PAM STAMP 2G for the three-rolling (0°, 45°, 90°) directions by incorporating the obtained mechanical properties tabulated in Table 4.3. From Fig. 4.17, it is clear that failure location and pattern is similar as experiment. After performing the simulations, the limit strains are identified for 0°, 45°, and 90° rolling directions as tabulated in Table 4.6.

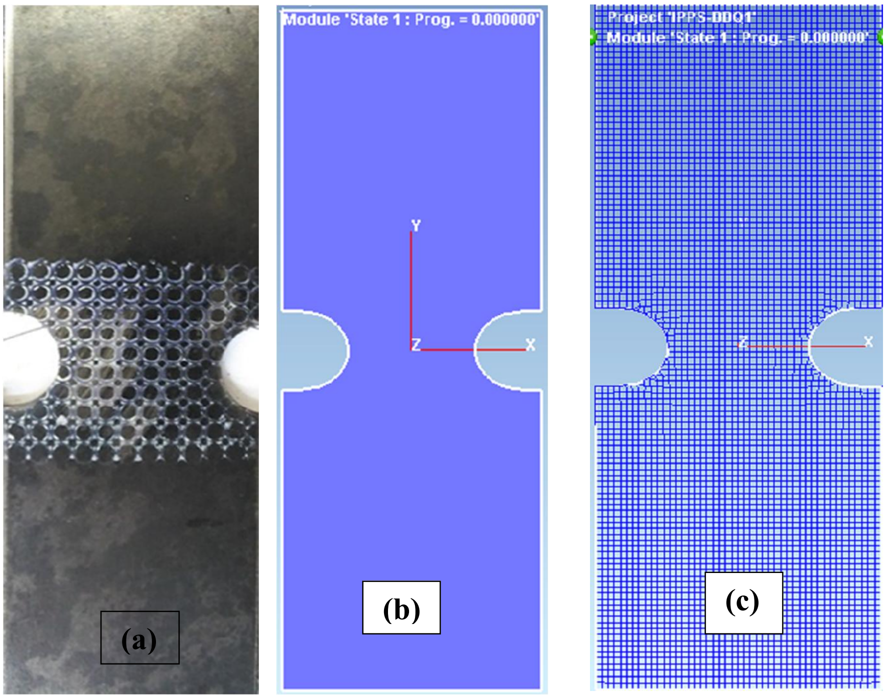

Figure 4. 8 In-plane plane-stretching specimens for (a) experiment (b) & (c) Solid CAD model and Meshed sample in PAM STAMP 2G before testing and simulation.

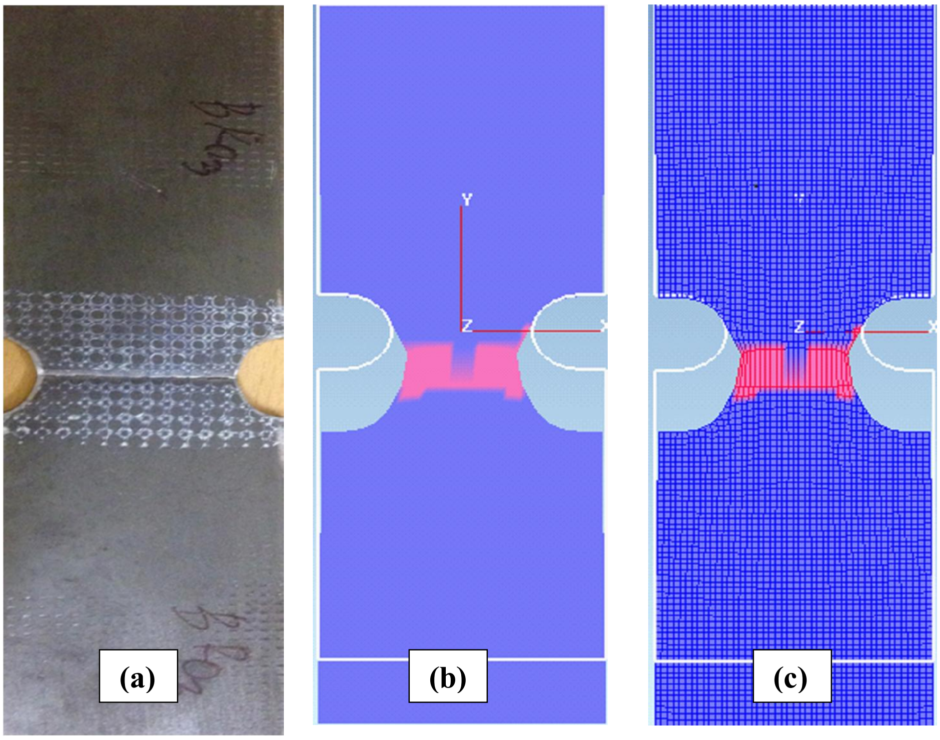

Figure 4. 97 In-plane plane-stretching specimens for (a) experiment (b) & (c) Solid CAD model and Meshed sample in PAM STAMP 2G after experimentation and simulation.

Table 4. 6 limit strains obtained from the Simulation

Rolling Direction	Major strain	Minor Strain
0°	0.204	0.116
45°	0.495	0.375
90°	0.354	0.287

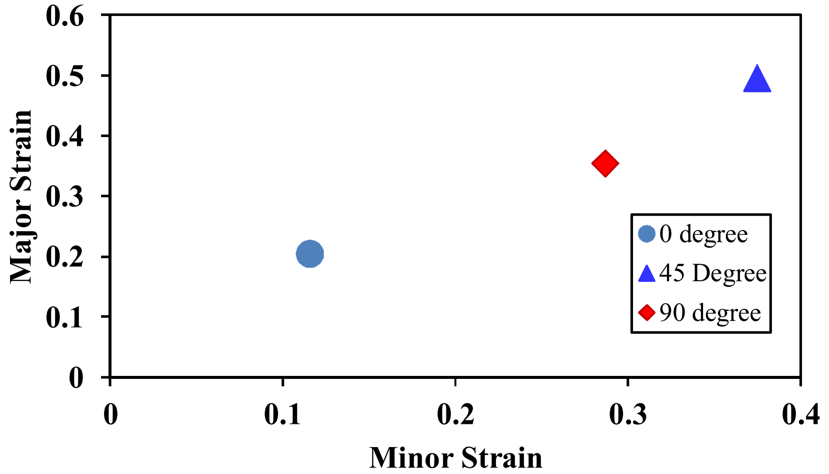

Figure 4. 10 Comparison of limit strains obtained from simulation of in-pane plane-stretching test on three rolling directions

Limit strain are evaluated using the TGNC after simulating on three rolling direction. The maximum limit strain is appeared for the rolling direction of 45° and followed by the 90° and 0° (Figure 4.18). This indicates that the maximum formability is in 45° rolling direction during in-plane plane-stretching test similar to experimentation.

Table 4. 7 Limit strains comparison between experiment and simulation results

Rolling Direction ⟹ Test ⟱	0°		45°		90°	
	Major Strain	Minor Strain	Major Strain	Minor Strain	Major Strain	Minor Strain
Experiment	0.188	0.109	0.517	0.365	0.386	0.3085
Simulation	0.204	0.116	0.495	0.375	0.354	0.287
Error	7.84%	6.03%	4.26%	2.67%	8.03%	6.97%

Table 4.7 shows the limit strain comparison between experiment and simulation results. From these results, it is matched with the experimental results with an acceptable error percentage of 5 to 8 % as per the standards.

From the obtained results and discussion of formability of EN - 10492-2 through in-plane plane-stretching test and also basic mechanical tests for three rolling directions of the sheets, it is interrelated that formability of the EN - 10492-2 steel sheet has more forming ability along 45° rolling direction among 0° and 90° rolling direction. It is can be derived from the mechanical properties and forming limit strains obtained from IPPS condition from experiments and simulations. The majorly strain hardening exponent (n) and plastic strain ratio (R) are deciding factors for sheet metal formability. This EN-10492-2 steel sheet has more plastic strain ratio (R) in 45° rolling direction and has almost equal value of strain hardening exponent (n) to 0° and 90° rolling direction. These factors lead to more formability in 45° rolling direction of the sheet.

CHAPTER FIVE

5. Conclusions and Recommendations

5.1. Conclusions

In this thesis work, In-plane Plane stretching test is analysed in order to determine limit strains of the EN-10149 S700mc) steel material. For determination of limit strains, the material was tested under three rolling directions. Moreover, the effect of rolling direction to the plain stretching test also studied. From this work, the following conclusions are drawn and summarized as follows:

- EN-10149 02 (S700mc) steel materialhad the highest yield and tensile strength at the Transverse direction (90°) and at diagonal direction (45°).The strain hardening exponent and total % elongation is more at the 0°and decreases in diagonal direction (45°).
- The microstructure result shows that the material constitutes more perlite matrix grain structure with small carbide boundaries. Therefore, these results indicate that the material is more ductile and formable. Vickers's hardness ofEN-10149 S700mc) steel materialvalue is 124.94 VHN.
- In-Plane Plane stretching experimental tests the limit strain evaluated using the TGNC after experiment on three rolling direction. The maximum limit strain is appeared for the rolling direction of 45° and followed by the 90° and 0°. This indicates that the maximum formability is in 45° rolling direction during in-plane plane-stretching test.
- The simulation results of limit strains show that the major limit stain is in 45° rolling direction during in-plane plane-stretching test similar to experimentation.
- It is observed that both experimental and Simulation results are with an acceptable error percentage of 5 to 8 % as per the standards.

5.2. Recommendations

The following recommendations are point out from the study:

- It is recommended that IPPS sample geometry should be modified to provide more clamping surface for the grips to hold the sample. This may provide more consistent failure of the sheet samples during testing.
- A camera with a higher capture rate and medium to high resolution could be used to better capture the local forming limits of the EN-10149-2 (S700mc) steels.

5.3. Future workcould be applied to future work in this area

- It is recommended that better study the macrostructure and limit strain of the material at different heat treated temperature.
- Additional work should be conducted to look at the strain rate effect in IPPS tests using strain rates that more closely match those employed in real-world.
- A more detailed (microstructures) study should be conducted to determine why the material failed at such a low strain level in 00rolling direction during the IPPS tests.

REFERENCE

[1]. Handbook, A. S. M. (2006). Volume 14B Metalworking: Sheet Forming. ASM International, 924.

[2]. Handbook, A. M. (1993). Vol. 14 Forming and Forging. ASM international.

[3]. Panich, S., Barlat, F., Uthaisangsuk, V., Suranuntchai, S., & Jirathearanat, S. (2013). Experimental and theoretical formability analysis using strain and stress based forming limit diagram for advanced high strength steels. Materials & Design, 51, 756-766.

[4]. Garcia, C. I. (2017). High strength low alloyed (HSLA) steels. In Automotive Steels (pp. 145-167).

[5]. http://automotive.arcelormittal.com/europe/products/HYTSS/HSLA/EN Automotive Worldwide.

[6]. Banabic, Dorel (2010). Sheet metal Forming process and constitutive Modeling and numerical simulation (pp.142 -144) Springer, Dordrecht London, Heidelberg. New York

[7]. Eary DF (1974). Techniques of press working sheet metals. Prentice Hall, London.

[8]. Keeler, S. P., & Backofen, W. A. (1963). Plastic instability and fracture in sheets stretched over rigid punches. Asm Trans Q, 56(1), 25-48.

[9]. Goodwin, G. M. (1968). Application of strain analysis to sheet metal forming problems in the press shop. SAE Transactions, 380-387.

[10]. Ozturk, F., & Lee, D. (2005). Experimental and numerical analysis of out-of-plane formability test. Journal of Materials Processing Technology, 170(1-2), 247-253.

[11]. Holmberg, S., Enquist, B., & Thilderkvist, P. (2004). Evaluation of sheet metal formability by tensile tests. Journal of Materials Processing Technology, 145(1), 72-83.

[12]. Keeler, S. P. (1968). Circular grid system—a valuable aid for evaluating sheet metal formability. SAE Transactions, 371-379.

[13]. Lee, R. S., & Hsu, Q. C. (1994). Image-processing system for circular-grid analysis in sheet-metal forming. Experimental mechanics, 34(2), 108-115.

[14]. Wang, C. C., Lee, J., Chen, L. W., & Lai, H. Y. (2000). A new method for circular grid analysis in the sheet metal forming test. Experimental Mechanics, 40(2), 190-196.

[15]. Safari, M., Hosseinipour, S. J., & Azodi, H. D. (2011). Experimental and numerical analysis of forming limit diagram (FLD) and forming limit stress diagram (FLSD). Materials Sciences and Applications, 2(05), 496.

[16]. Keeler, S., & Kimchi, M. (2015). Advanced high-strength steels application guidelines V5. WorldAutoSteel.

[17]. Marziniak, Z., & Kuczynski, K. (1967). Limit strain in the process of stretch-forming sheet metals. Int. J. Mech. Sci,9(9), 609-620.

[18]. Brozzo, P., Deluca, B., & Rendina, R. (1972, October). A new method for the prediction of formability limits in metal sheets. In Proc. 7th biannual Conf. IDDR.

[19]. Lewison, D. J., & Lee, D. (1999). Determination of forming limits by digital image processing methods (No. 1999-01-3168). SAE Technical Paper.

[20]. Hecker, S. S. (1975). Simple technique for determining forming limit curves. Sheet Metal Industries, 52(11), 671-676.

[21]. Goodwin, G. M. (1968). Application of strain analysis to sheet metal forming problems in the press shop. SAE Transactions, 380-387.

[22]. Raghavan, K. S. (1995). A simple technique to generate in-plane forming limits curves and selected applications. Metallurgical and materials transactions A, 26(8), 2075-2084.

[23]. Ghosh, A. K., & Hecker, S. S. (1974). Stretching limits in sheet metals: in-plane versus out-of-plane deformation. Metallurgical Transactions, 5(10), 2161-2164.

[24]. R. H Wagoner. (1980) "Measurement and Analysis of Plane-Strain Work Hardening," Metallurgical Transactions A, 11A: pp. 165-175,

[25]. Wagoner, R. H., & Laukonis, J. V. (1983). Plastic behavior of aluminum-killed steel following plane-strain deformation. Metallurgical Transactions A, 14(7), 1487-1495.

[26]. Laukonis, J. V., & Wagoner, R. H. (1985). Plastic behavior of dual phase steel following plane-strain deformation. Metallurgical Transactions A, 16(3), 421-425.

[27]. Lee, R. S., & Hsu, Q. C. (1994). Image-processing system for circular-grid analysis in sheet-metal forming. Experimental mechanics, 34(2), 108-115.

[28]. Wang, Y. D., Xu, S. H., Ren, S. B., & Wang, H. (2016). An experimental-numerical combined method to determine the true constitutive relation of tensile specimens after necking. Advances in Materials Science and Engineering, 2016.

[29]. Nandedkar, V. M. (2000). Formability studies on a deep drawing quality steel (Doctoral dissertation, Ph. D. thesis, IIT Bombay, Mumbai, India).

[30]. Hill, R. (1998). The mathematical theory of plasticity (Vol. 11). Oxford university press.

[31]. Hollomon, J. H. (1945). Tensile deformation. Aime Trans, 12(4), 1-22.

[32]. Hill, R. T. (1952). On discontinuous plastic states, with special reference to localized necking in thin sheets. Journal of the Mechanics and Physics of Solids, 1(1), 19-30.

[33]. Keeler, S. P., & Brazier, W. G. (1977). Relationship between laboratory material characterization and press-shop formability. In Proc. Conf. on Micro alloying 75, 1977, 517-528.

[34]. Keeler, S. P. (1971). Understanding Sheet-Metal Formability. Pt. 1. State of The Art. Sheet Metal Ind, 48(5), 357-361.

[35]. Burke, J. J., & Weiss, V. (2012). Advances in deformation processing. Springer Science & Business Media.

[36]. Wagoner, R. H., & Wang, N. M. (1979). An experimental and analytical investigation of in-plane deformation of 2036-T4 aluminum sheet. International Journal of Mechanical Sciences, 21(5), 255-264.

[37]. https://bodybuilderhomepage.scania.com/index.aspx.

[38]. http://www.victorsteel.net/en-10149-2-EN-10149-2 (S700mc)-steel-plate.html

[39]. ASTM American Society for Testing and Materials. (2009).Standard test methods for tension testing of metallic materials. ASTM international.

[40]. Devenpeck, M. L., & Richmond, O. (1982). Limiting Strain Tests for In-Plane Sheet Stretching. Novel Techniques in Metal Deformation Testing, 79-88.

[41]. Sang, H., & Nishikawa, Y. (1983). A plane strain tensile apparatus. JOM, 35(2), 30-33.

[42]. Kim, H. J., & Lee, D. (1996). Further development of experimental methods to verify computer simulations. Proceedings of NUMISHEET, Dearbom, Michigan, USA, 316-323.

[43]. Ozturk, F., Dilmec, M., Turkoz, M., Ece, R. E., & Halkaci, H. S. (2009, June). Grid marking and measurement methods for sheet metal formability. In 5th International Conference and Exhibition on Design and Production of MACHINES and DIES/MOLDS (pp. 18-21).

[44]. Hariharan, K., & Balaji, C. (2009). Material optimization: A case study using sheet metal-forming analysis. Journal of materials processing technology, 209(1), 324-331.

[45]. Mäntyjärvi, K., Tulonen, J., Saarnivuo, T., Porter, J., & Karjalainen, J. A. (2008). Grid patterns by laser for forming strain analysis. International Journal of Material Forming, 1(1), 249-252.

[46]. Joshi, A. M. (2002). Strain studies in sheet metal stampings. BE Mechanical, AMI Prod.

[47]. Li, D., & Ghosh, A. (2003). Tensile deformation behavior of aluminum alloys at warm forming temperatures. Materials Science and Engineering: A, 352(1-2), 279-286.

[48]. Demeri, M. Y. (2006). Forming of Advanced High Strength Steels, ASM Handbook; Vol. 14B; Metalworking: Sheet Forming, Semiatin, SL, ed. ASM International, Materials Park, OH. USA.

[49]. Hill, R. (1948). A theory of the yielding and plastic flow of anisotropic metals. Proc. R. Soc. Lond. A, 193(1033), 281-297.

[50]. Langford, W. F., Snyder, S. C., & Bausch, J. (1950). New Criteria for Predicting the Press Performance of Deep Drawing Steels. Trans, Amer. Soc. Metals, 42, 1197-1232.

[51]. Agnew, S. R., & Duygulu, Ö. (2005). Plastic anisotropy and the role of non-basal slip in magnesium alloy AZ31B.International Journal of plasticity, 21(6), 1161-1193.

[52]. Drewett, L., Bremer, S., Liebeherr, M., De Waele, W., Martin-Meizoso, A., Brozda, J., & Gubeljak, N. (2010). HIPERC: a novel, high performance, economic steel concept for linepipe and general structural use. Publications office of the European Union.

Appendix: -A Circular Grid stamp complete Drawing

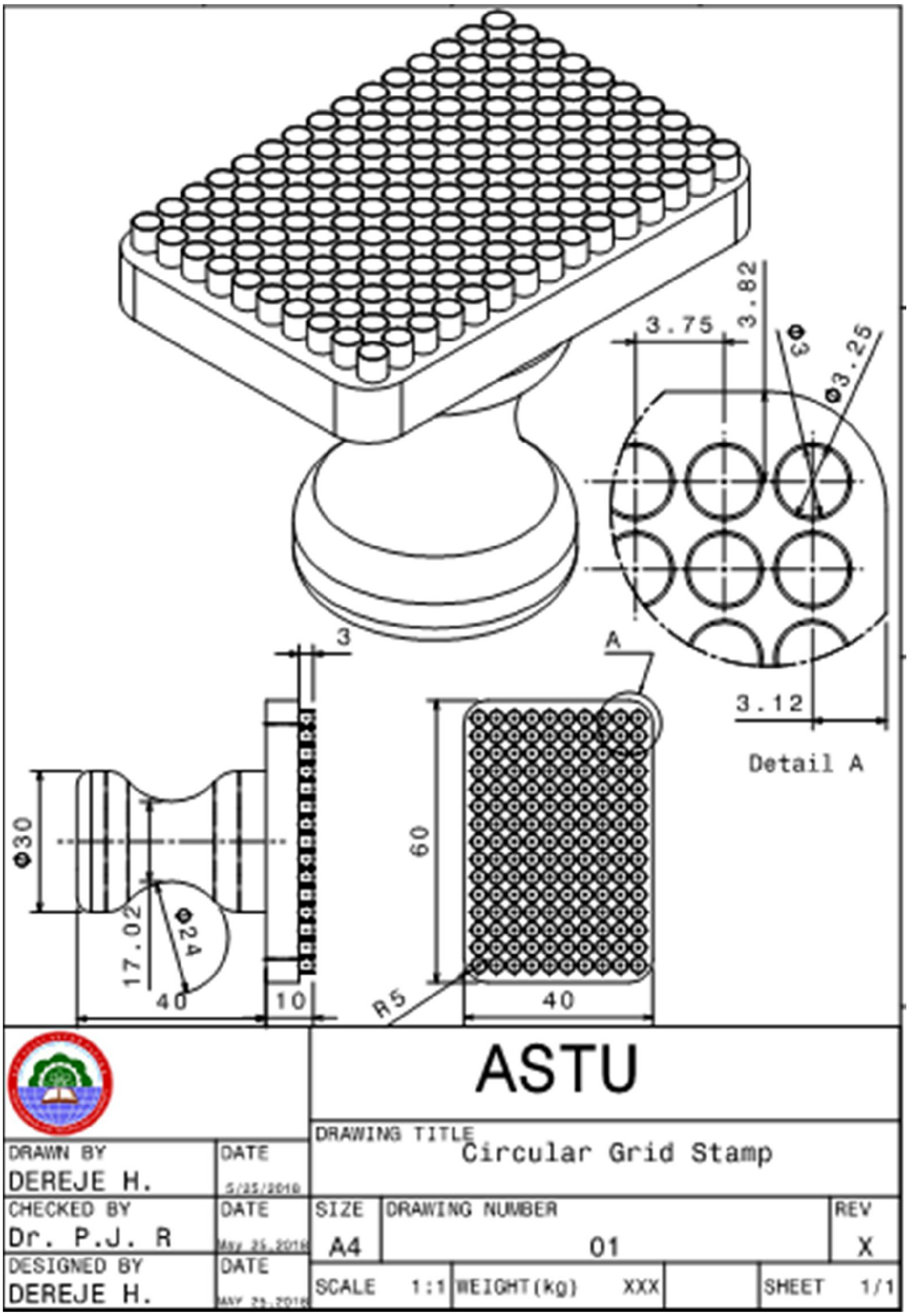

Appendix: - B Sample prepared for microstructure and hardnesss testiting